UNIVERSITY OF CALIFORNIA, SAN DIEGO

Rapid and dynamic growth of Arabidopsis seedlings in response to changes in light quality: A live imaging study

A dissertation submitted in partial satisfaction of the requirements for the degree Doctor of Philosophy

in

Biology

by

Benjamin Jeremy Cole

Committee In Charge:

Professor Joanne Chory, Chair
Professor Steve A. Kay, Co-Chair
Professor Joseph R. Ecker
Professor James Golden
Professor Alexander Hoffmann

2011

The Dissertation of Benjamin Jeremy Cole is approved, and it is acceptable in quality and form for publication on microfilm and electronically:

_____

_____

_____

_____
Co-Chair

_____
Chair

University of California, San Diego

2011

DEDICATION

I dedicate this thesis to my loving parents, Susan and Philip, whose support and encouragement always seemed to make the long way across the country. To my gracious advisor and co-advisor, Joanne and Steve, for being the tremendous resources they are, and helping me to find my academic footing. And lastly, to Dana, for making my life interesting and exciting, even at the most perilous dips in the graduate school rollercoaster.

TABLE OF CONTENTS

LIST OF OF FIGURES AND TABLES

ACKNOWLEGEMENTS

I would like to acknowledge my thesis advisor, Joanne Chory, my co-advisor, Steve Kay, and the rest of my thesis committee (Joe Ecker, Alex Hoffmann, James Golden, and Robert Schmidt) for their generous support and guidance of my scientific development. I would also like to thank all the members of the Plant Biology Laboratory at the Salk Institute for invaluable advice and support through the incalculable rigors of graduate school.

Portions of Chapter 1 is taken from a study which was conducted by Chen, Kunhua; Cole, Benjamin; Gregory, Brian; Ecker, Joeseph; and Chory, Joanne, 2007

Chapter 2 is a reproduction in full of the material as it appears in The Plant Journal, 2011. Cole, Benjamin; Kay, Steve A.; Chory, Joanne. Blackwell Publishing Ltd., 2011. The dissertation author was the primary investigator and author of this paper.

Chapter 3, in part, is being prepared for submission for publication of the material Cole, Benjamin J., Jaillais, Yvon, Kay, Steve A., Chory, Joanne. The dissertation author was the primary investigator and author of this material.

Appendix A, in part, has been submitted for publication of the material as it may appear as a book chapter in Methods in Molecular Biology, 2011; Cole, Benjamin J., Chory, Joanne. Humana Press 2011.

VITA

2005 Intern, Boyce-Thompson Institute of Plant Research

2006 Bachelor of Sciences, Rensselear Polytechnic Institute

2011 Doctor of Philosophy, University of California, San Diego

PUBLICATIONS

Cole, B., and Bystroff, C. “Alpha-Helical Crossovers favor right-handed supersecondary structures by kinetic trapping. The phone cord effect in protein folding” (2009). Protein Science 8: 1602-1608.

Cole, B., Kay, SA., and Chory, J. “A dynamic analysis of hypocotyl growth during shade avoidance in Arabidopsis.” (2011) The Plant Journal 65:991-1000.

FIELDS OF STUDY

Major Field: Biology

Studies in Computational Biology
Professor Christopher Bystroff

Studies in Plant Biology
Professors Joanne Chory and Steve Kay

ABSTRACT OF THE DISSERTATION

Rapid and dynamic growth of Arabidopsis seedlings in response to changes in light quality: A live imaging study

by

Benjamin Jeremy Cole

Doctor of Philosophy

University of California, San Diego, 2011

Professor Joanne Chory, Chair

Professor Steve A. Kay, Co-Chair

Light governs plant life both as an energy source and as an information cue, and regulates virtually every aspect of plant growth and development from seed to senescence. This dissertation examines the role of light as a source of information in regulating early seedling development. Specifically, the role of chromatin modification in light-regulated photomorphogenesis in *Arabidopsis thaliana* was studied using a mutant, *det1-1*, which undergoes premature photomorphogenesis in darkness. Global DNA de-

methylation was observed from whole-genome tiling arrays in *det1-1* in comparison to wild-type, yet this phenotype was insufficient to explain the suite of defects associated with the *det1-1* mutation, and the mechanistic details of how these changes come about are still unclear. A similar role by light in changing plant architectural development is exemplified by the shade avoidance syndrome, where plants attempt to evade vegetative shade by reallocation of energy towards apical growth. Hypocotyl (the embryonic stem) elongation is one feature which is altered dramatically in response to shade, and this phenotype was measured with unbiased temporal precision through a novel image-based assay and accompanying software. Using this tool to measure hypocotyl length in time-resolved image stacks, hypocotyls were shown to have a dynamic multi-phasic growth pattern in response to shade, which consisted of an initiation elongation phase, followed by a period of slower growth, and finally a second major elongation phase, all occurring over a period of 10 hours. New biosynthesis of the phytohormone, auxin, was demonstrated to have a clear role in the initiation of this dynamic growth pattern, which was reflected at the level of transcriptional regulation. Another hormone, brassinosteroid, and the signal transduction pathway following its synthesis and perception was also investigated and found to have a role in regulating shade-induced elongation. When brassinosteroid perception was impared, seedlings failed to resume elongation growth after the slowing phase following shade exposure, and modulation of endogenous brassinosteroid signaling components in wild-type seedlings was also apparent, implying a role for brassinosteroid regulation in controlling the observed growth patterns. Thus, multiple light and hormone signaling pathways must integrate environmental cues to initiate appropriate responses to adverse conditions.

INTRODUCTION

Light is one of the most abundant energy sources on the planet. It provides the energy for fixation of atmospheric carbon dioxide to usable carbohydrates during photosynthesis, a process shared by all plant and much of microbial life. Indeed, one enzyme critical for photosynthesis, RuBisCO (Ribulose 1,5 Bisphosphate carboxylase/oxygenase), has been estimated to be the most abundant enzyme on earth. Plants, as autotrophs, almost exclusively depend on light for growth. Light not only serves to fuel carbon assimilation and growth, but also to inform plants (incapable of moving away from adverse conditions) to their surroundings, prompting architectural, physiological, and molecular changes as part an incredible potential for adaptative plasticity. The study of how light is utilized by plants for both of these purposes has never been more pertinent than today, since humans (now as a population of 7 billion) are almost entirely dependent on photosynthetic life for our own nutrition (UNFPA, 2011), and must adapt our food resources if we wish to maintain this population into the future (Premanandh, 2011). In studying plants, many researchers have turned to a genetic model system, *Arabidopsis thaliana*, a small member of the mustard family, which has a rapid life cycle (~10 weeks from seed to seed) and diploid genetics, reproduces almost entirely via self-fertilization, and has very simple growth requirements. Importantly, the *Arabidopsis* genome has been fully sequenced, and (in addition to the ever-growing collection of mutant lines isolated from traditional genetic screens) a huge variety of computational and reverse genetics/genomics tools exist, making global-scale phenotyping possible.

The life cycle of a widely used population of Arabidopsis, Columbia-0 (Col-0) has

been very well characterized. Arabidopsis starts off as a double-fertilization event of an ovule and two sperm which are typically introduced to the ovaries from pollen derived from the same flower (self-fertilization). Embryonic development is then initiated, transitioning through various stages during which patterning of two cotyledons, a hypocotyl, and an embryonic root is established. This embryo is encased in a seed, and released away from the mother plant now undergoing senescence. When water is imbibed, germination is initiated, and (if the seed is buried, or occluded from light) the hypocotyl (connecting the root and the shoot) beings elongation growth (etiolated growth, or skotomorphogenesis), pushing the cotyledons (containing the photosynthetic machinery) above the soil surface. When light is encountered, hypocotyl growth is rapidly terminated, the cotyledons unfold and expand, and chlorophyll is synthesized to begin photosynthesis (a process called de-etiolation, or photomorphogenesis). True leaves are developed from the shoot apical meristem (a collection of stem cells at the apex of the hypocotyl). These leaves form a rosette pattern, characteristic of the vegetative stage of development, where the plant is mostly accumulating carbon reserves and expanding. Growth during the vegetative stage can often be threatened by shading conditions of high density ecosystems (manifested as an alteration in the light quality) – *Arabidopsis* can detect this change, and initiate elongation of its petioles (connective tissue between the leaves and shoot-apical meristem), hypocotyl, and leaves, in an effort to position its photosynthetic organs to optimally perceive light. Under short-day conditions (during winter months, when reproductive success is unlikely), this vegetative growth pattern continues until the photoperiod becomes longer (during the summer months), triggering inflorescence stems to bolt from the shoot-apical meristem, and initiating floral production. This transition to the reproductive phase of the life cycle is terminal in *Arabidopsis thaliana*; soon after all new flowers are produced, the

plant self-fertilizes, sets seeds, and dies.

As mentioned above, light influences nearly every aspect of plant development. Plants have evolved a sophisticated suite of photosensory molecules capable of relaying quantitative and qualitative information from the light environment to elicit an appropriate response. One of the first class of these molecules to be identified, phytochromes, were first purified as a "photoreversible pigment" from turnip seedlings; absorbing a red light photon (at 660 nm) converted this pigment to a far-red light absorbing form, and vice versa (Butler et al., 1959). Since this seminal discovery, *Arabidopsis* hypocotyls have emerged as the model of choice in studying light regulation of plant growth, due to its simple structure, extreme sensitivity to growth regulators (including light), and preference to grow by longitudinal cell expansion rather than by cell proliferation (Gendreau et al., 1997). Using genetic screens in *Arabidopsis* for hypocotyls which are elongated red (R), far-red (FR), or blue (B) light, many genes encoding photoreceptors responsible for light-regulated growth have been identified, including the red light phytochrome photoreceptors, (*PHYTOCHROME A* and *PHYTOCHROME B*; *PHYA and PHYB*), as well as the blue-light cryptochrome photoreceptors, *CRYPTOCHROME 1* (*CRY1*) and *CRY2* (Ahmad and Cashmore, 1993; Nagatani et al., 1993; Reed et al., 1993). Additional screens for *Arabidopsis* mutants which cannot bend towards low-fluence unidirectional light during skotomorphogenesis (a process termed phototropism) have identified additional blue-light photoreceptors, *PHOTOTROPISM 1* (*PHOT1*) and *PHOT2* (Liscum and Briggs, 1995; Christie et al., 1998; Briggs et al., 2001). Thus, plants possess the capability to sense information from a broad range of the light spectrum, triggering physiological responses which optimally position light-harvesting organs to utilize this all-important resource, often in sub-optimal light conditions.

Much of recent work has been to characterize the structural basis of

photoperception, and how these signals are relayed to downstream effector molecules which modulate growth and development. Phytochromes have been extensively characterized, and have been shown to exist as distinct conformers, the Pr (red-light absorbing) and the Pfr (far-red light absorbing) form, with the latter being the more active form of the molecule (Rockwell et al., 2006; Yang et al., 2009). Upon conversion to Pfr via a light-initiated cis/trans isomerization event of the covalently attached chromophore, phytochromobilin and the ensuing protein conformational change (Lagarias and Rapoport, 1980; Rüdiger et al., 1983), phytochrome localizes to the nucleus (Sakamoto and Nagatani, 1996), where it forms nuclear speckles (Chen et al., 2005). Phytochrome A is light-labile, degrading quickly after conversion to the Pfr form. Phytochrome B, on the other hand, is more stable, and can interact with (and consequently target for degradation) a subclass of basic helix-loop-helix transcription factors, *PHYTOCHROME INTERACTING FACTOR 3* (*PIF1*), *PIF3*, *PIF4*, *PIF5*, *PIF6*, and *PIF7* which negatively regulate various aspects of phytochrome signaling (Ni et al., 1998, 1999; Huq and Quail, 2002; Khanna et al., 2004; Leivar et al., 2008).

One such aspect is repression of photomorphogenesis in the dark, which is also repressed by a set of regulators, whose founding member, *DE-ETIOLATED 1* (*DET1*) displays premature de-etiolation under dark conditions (Chory et al., 1989; Pepper et al., 1994). Subsequent screens for mutants exhibiting similar "DET" phenotypes properties identified numerous *CONSTITUTIVE PHOTOMOROPHOGENESIS* (COP) and *FUSCA* genes, the latter accumulating high anthocyanin levels in cotyledon tissue during embryogenesis and early seedling development, a feature shared by many COP and DET loci (Deng et al., 1991, 1992; Kwok et al., 1996). These *COP/DET/FUS* family of negative photomorphogenic regulators comprise at least three major protein complexes, the COP1 E3 ligase complex which is responsible for degradation of multiple light-

regulated signaling components, the COP9 signalosome, responsible for regulation of E3 ligase complexes involved in light signal transduction (Wei et al., 2008), and the CDD complex (composed of DET1, DDB1 encoded by *DAMAGED DNA BINDING PROTEIN 1*, and COP10) which has been implicated in chromatin regulation and transcriptional repression (Benvenuto et al., 2002; Yanagawa et al., 2004; Castells et al., 2011; Lau et al., 2011). However, despite decades of intense work to understand how COP/DET/FUS proteins repress photomorphogenesis, the exact mechanism by which this repression occurs remains elusive.

Apart from photomorphogensis, light (through photoreceptor signaling) is important for optimal growth in high density. The threat of shading by neighboring vegetation can be detected through shift in the amount of R to FR light (typically described by the R/FR ratio), as the chlorophyll in leaf tissue absorbs primarily in the R and B spectrum, yet reflects (or transmits) radiation in the FR spectrum, lowering the R/FR (Kasperbauer, 1987; Ballaré et al., 1990). This drop in R/FR triggers a suite of physiological changes, collectively known as the Shade Avoidance Syndrome, including a decrease in germination rate, hypocotyl, petiole, and leaf and internode elongation, early flowering, decreased root growth, decreased chlorophyll accumulation, and decreased defense capacity against herbivores (Smith and Whitelam, 1997; Izaguirre *et al.*, 2006; Moreno *et al.*, 2009; Franklin, 2008). Phytochrome is perfectly situated to perceive this shift, as the ratio between the Pfr and Pr form will mirror changes in the R/FR ratio (Smth and Holmes, 1977). Upon conversion to the Pfr form, phyB (the major phytochrome to regulate shade responses, along with phyD and phyE) binds to PIF4 and PIF5, targeting them to degradation via the 26S ubiquitin proteosome system (Franklin et al., 2003; Lorrain et al., 2008). When shading occurs (or is imminent), the R/FR drops, converting most phyB protein to the Pr form, releasing PIF4 and PIF5 from

repression. PIF4 and PIF5 can then modulate shade-regulated gene expression, though a direct impact of transcription on extension growth has not been demonstrated. Other PIFs have been postulated to redundantly control shade avoidance phenotypes, as *pif4pif5* double mutant seedlings still show shade responsiveness (Lorrain et al., 2008; Cole et al., 2011). Complicating the shade signal transduction pathway is massive up-regulation of putative negative regulators, *PHYTOCHROME INTERACTING FACTOR 3-LIKE 1* (PIL1), *LONG HYPOCOTYL IN FAR-RED 1* (HFR1), *PHYTOCHROME RAPIDLY REGULATED 1* (PAR1) and PAR2 (Salter et al., 2003; Sessa et al., 2005; Roig-Villanova et al., 2006), mutation of which cause slight hyper-responsiveness to shade, suggesting a negative feedback attenuating an out-of-control shade response.

Many of the genes which are regulated by shade are also regulated by the circadian clock (Michael et al., 2008), a 24 hour molecular oscillator consisting of multiple interlocking transcriptional feedback loops which generate cycling patterns of gene, protein, and metabolite accumulation (Doherty and Kay, 2010). Indeed, evidence from circadian regulation of *PIL1* transcript accumulation and *EARLY FLOWERING 3* (ELF3, a core circadian clock component) complex regulation of *PIF4* and *PIF5* gene expression has implicated the circadian clock in gating shade responses (Salter et al., 2003; Nozue et al., 2007; Nusinow et al., 2011). This gating of shade responses by the clock could represent a modulation of sensitivity to shade at times of day when it is most likely to be perceived, as the morning and evening light environments are enriched for FR light, making the R/FR shift all the more apparent at low solar angles, amplified by heliotropic movement of neighboring leaves (Kasperbauer, 1987). Regardless the ecological considerations as to why circadian gating exists, careful attention must be paid in experimental settings that sampling of molecular or physiological phenotypes occurs at the correct time of the day.

In addition to phytochrome regulation of PIF levels, phytohormone signaling is also critically important for shade signal transduction. In *Arabidopsis*, at least eight major hormones have been identified, including auxin, brassinosteroid (BR), gibberelic acid (GA), and ethylene (ET), among others. The major signaling pathways have now been characterized for the aforementioned hormones. Auxin binds to a receptor, *TRANSPORT INHIBITOR RESISTANT 1* (TIR1), which (as part of an E3 ubiquitin ligase complex) triggers proteosomal degradation of a set of *Aux/IAA* (IAA) regulators, themselves inhibiting *AUXIN RESPONE FACTOR* (ARF) transcription factors from modulating the auxin transcriptional response (Chapman and Estelle, 2009). The auxin biosynthetic pathway consists of at least two enyzmatic reactions: conversion of tryptophan to indole-3-pyruvic acid (IPA) via *TRYPTOPHAN AMINOACID TRANSFERASE 1* (TAA1; also known as *SHADE AVOIDANCE 3* or SAV3), and conversion of IPA to indole-3-acetic acid (IAA, or auxin) via the *YUCCA* family of flavin monooxygenases (Zhao et al., 2001; Stepanova et al., 2008; Tao et al., 2008; Mashiguchi et al., 2011; Won et al., 2011). Rapid new synthesis of auxin is critical for proper shade avoidance responses, as mutation of *sav3* nearly eliminates any seedling shade avoidance phenotype (Tao et al., 2008). Furthermore, up-regulation of several auxin-regulated genes also occurs during shade avoidance, among them many of the IAA genes (e.g. *IAA19* and *IAA29*), *ARABIDOPSIS THALIANA HOMEODOMAIN BOX 2* (ATHB-2), and *HOMEOBOX OF ARABIDOPSIS THALIANA 2* (HAT2) (Carabelli et al., 1996; Steindler et al., 1999; Tao et al., 2008). However, the mechanistic details of how light signaling can regulate auxin levels during shade avoidance is still unclear.

Gibberelic acid, ethylene, and brassinosteroids also have demonstrated roles in mediating shade avoidance responses. GA mediates interaction between *GIBBERELLIN INSENSITIVE DWARF 1* (GID1) and five DELLA-domain containing

proteins, targeting the DELLA proteins (which repress growth in the absence of GA) for degradation (Schwechheimer and Willige, 2009). DELLA protein levels in Arabidopsis petioles are reduced in response to low R/FR, and shade responsiveness is reduced when GA biosynthesis is impaired (Djakovic-Petrovic et al., 2007). Furthermore, DELLA proteins can interact with (and inhibit) PIF3 and PIF4, which provides evidence of a link between phytochrome and gibberellic acid signaling (de Lucas et al., 2008; Feng et al., 2008). Ethylene signals by binding to (and inhibiting) its receptors, *ETHYLENE RESPONSE 1* (*ETR1*), *ETR2, ETHYLENE RESPONSE SENSOR 1* (*ERS1*), *ERS2*, and *ETHYLENE INSENSITIVE 4* (*EIN4*), which together with a copper-containing protein, *CONSTITUTIVE TRIPLE RESPONSE 1* (*CTR1*) negatively regulate downstream responses, including a transcription factor *EIN3* which is proposed to modulate ET-induced transcriptional responses (Stepanova and Alonso, 2009). Ethylene is another positive regulator of shade responses, as exogenous application of an ethylene precursor, 1-aminocyclopropane-1-carboxylic acid (ACC) stimulated hypocotyl elongation similar to that caused by low R/FR, ethylene production is increased in response to shade, and mutation of ethylene signaling components abolished shade responsiveness (Pierik et al., 2009). Brassinosteroid signaling has also been well-characterized, consisting of a linear pathway where BR binds its receptor, *BRASSINOSTEROID INSENSITIVE 1* (BRI1), facilitating interaction with and activation of a second receptor-like kinase, *BRI1-ASSOCIATED KINASE 1*, and disrupting interaction with an unstructured inhibitor, *BRASSINOSTEROID KINASE INHIBITOR 1* (BKI1), resulting in a fully active receptor complex (Li and Chory, 1997; Friedrichsen et al., 2000; He et al., 2000; Wang and Chory, 2006; Hothorn et al., 2011; Jaillais et al., 2011). This complex phosphorylates and activates *BR SIGNALING KINASE 1* (BSK1), which in turn activates the phosphatase, *BRI1 SUPPRESSOR 1* (BSU1) (Kim et al.,

2009). BSU1 dephosphorylates and inactivates *BRASSINOSTEROID INSENSITIVE 2* (BIN2), which phosphorylates and inhibits downstream transcription factors, BES1 and BZR1 (Li et al., 2001; Nam and Li, 2002; Yin et al., 2002; Zhao et al., 2002). Brassinosteroids have not been characterized to have a role in regulating low R/FR responses, however similar responses to a different form of light-quality shade cue, reduction in blue light, is BR-dependent (Kozuka et al., 2010; Keller et al., 2011; Lian et al., 2011). Thus, shade avoidance employs multiple hormones, which likely interact with each other and with the light signaling pathways downstream of the photoreceptors, adding greatly to the complexity of shade signaling (Jaillais and Chory, 2010).

This enormous complexity of multiple signaling pathways involved in light regulated phenotypes inspired development of novel phenotyping tools which can separate physiological responses on a temporal scale. The first of these methods were developed for measuring growth kinetics of *Sinapis alba* stem elongation through usage of a Linear Voltage Displacement Transducers (LVDTs), which physically measure extension by attaching growing tissue to a string with a counterweight, and measuring displacement as the counterweight moves downward (Morgan et al., 1980; Child and Smith, 1987). These kinetic studies first indicated phytochrome growth regulation to be dynamic, existing in two distinct phases. Other studies in *S. alba* and Arabidopsis have demonstrated that multiple photoreceptors control hypocotyl growth inhibition during photomorphogenesis, and that these photoreceptors often act sequentially in mediating this inhibition (Cosgrove, 1982; Parks et al., 1998; Parks and Spalding, 1999). Recent technological advances in imaging and image processing have enabled more non-invasive phenotyping platforms for studying morphological properties of plants with unbiased precision (Miller et al., 2007; Wang et al., 2009). Studies employing this new technology have characterized non-redundant roles for blue light receptors in modulating

hypocotyl growth inhibition, a hallmark of photomorphogenesis (Miller et al., 2007). However, the present image processing algorithms are limited to measuring etiolated hypocotyl elongation, which is not well suited for shade avoidance studies. This dissertation highlights a potential new role of DET1 in regulating DNA methylation during repression of photomorphogenesis. A novel phenotyping platform for imaging and automatically measuring light-grown (fully de-etiolated) Arabidopsis seedling hypocotyls as elongation is promoted by exposure to shade conditions. This growth promotion is shown to be multi-phasic, initiated by new auxin biosynthesis, yet only partially mediated by PIF4 and PIF5 function. Lastly, a novel role for brassinosteroid biosynthesis and signaling in regulating hypocotyl elongation in low R/FR conditions is defined. High resolution temporal)along with tissue- and cell-type specific) studies will likely prove invaluable in separating complex multifaceted signal transduction pathways regulating any physiological process, as our models of plant growth and development continue to become more complete.

CHAPTER 1

Whole-Genome Analysis of Methylation Changes caused by mutation of DET1

Kunhua Chen, Benjamin J. Cole, Brian D. Gregory, Joespeh Ecker, and Joanne Chory

Abstract

Correct timing of photomorphogenesis is a critical aspect of early plant development, and is regulated in part by a protein complex containing DET1. Mutations in DET1 cause severe pleiotropic phenotypes, the hallmark of which is premature de-etiolation in darkness. Here, we describe differences between *det1-1* and wild-type chromatin at the methylation level. We describe *det1-1* to be slightly de-methylated across much of the genome, resulting in mis-regulation of genes involved in defense. These changes do not correlate strongly with differential expression of light-regulated genes, nor does exogenous treatment with non-methylatable cytosine recapitulate the DET phenotype in wild-type seedlings, even at high doses. We conclude that while DET1 may be involved in chromatin stability, this role is likely indirect.

Introduction

Light, the primary energy source for photosynthetic life, also yields valuable information about the environmental surroundings that land plants (firmly rooted to the ground) find themselves in. This aspect of light as an information source is especially important during the process of germination, when a plant transitions from reliance on seed energy stores to its own photosynthetic machinery for continued growth in light-rich conditions. When a seed germinates underneath the soil, it undergoes an etiolated growth pattern, by which the hypocotyl (the embryonic stem connecting basal and apical tissues) rapidly elongates to optimally position photosynthetic tissues (i.e. the cotyledons and petioles) to intercept light above the soil. Meanwhile, these photosynthetic tissues remain undeveloped and folded by an apical hook, which serves to protect the young seedling from physical stress associated with pushing above the ground. Upon light perception, photomorphogensis (or de-etiolation) occurs, where the photosynthetic machinery develops, the cotyledons unfold and expand, and the hypocotyl ceases to grow. Linking photomorphogenesis to light perception is critical, as premature de-etiolation beneath the surface could result in catastrophic damage to the seedling, and would prevent photosynthetic success.

The mechanisms by which photomorphogenesis occurs have been extensively studied for many decades (Chen et al., 2004). Phytochromes and cryptochromes (light receptors) were identified as positive regulators of light signaling from genetic screens for seedlings that cannot undergo photomorphogenesis in red or blue light conditions (Ahmad and Cashmore, 1993; Nagatani et al., 1993; Reed et al., 1993). These photoreceptor proteins transduce light information to elicit morphological changes, such as hypocotyl growth inhibition, apical hook unfolding, and cotyledon development. Conversely, other genetic screens have identified genes which prevent

photomorphogenesis under dark conditions (Chory et al., 1989; Deng et al., 1991, 1992; Pepper et al., 1994). Plants lacking functional products from these genes undergo ectopic photomorphogenesis in the dark, accumulate excessive anthocyanin pigment (indicative of high light stress), are dwarfed in stature, flower early, and set few seeds under light conditions. The first (and one of the more enigmatic) genes identified by these latter screens, *DE-ETIOLATED 1* (DET1) lacks any known functional domain, yet is conserved in most higher eukaryotes, localizes to the nucleus, and affects expression of a vast number of light-regulated genes (Schroeder et al., 2002). Another gene, *CONSTITUTIVE PHOTOMORPHOGENESIS 1* (COP1) encodes an RING E3 Ubiquitin Ligase with a WD-40 protein-protein interaction domain, and acts downstream of both blue- and red-light photoreceptors to repress photomorphogenesis in the dark (Deng et al., 1991; von Arnim and Deng, 1993; Ang and Deng, 1994).

Much of the more recent work to characterize these negative regulators of photomorphogenesis has been to establish the composition of the protein complexes they participate in, and what (if any) enzymatic function they exhibit. COP1 interacts with and mediates degradation of multiple light-regulated transcription factors, including transcriptional regulators, *LONG HYPOCOTYL 5* (HY5) (Osterlund et al., 2000), and *LONG HYPOCOTYL IN FAR-RED* (HFR1) (Yang et al., 2005), as well as the photoreceptor, *PHYTOCHROME A* (PHYA) (Seo et al., 2004). The mechanism by which COP1 responds to light has been suggested to involve competition between COP1 and CRY1 for binding of *SUPPRESSOR OF PHYA* (SPA1), a protein necessary for COP1 function (Lian et al., 2011; Liu et al., 2011). DET1, although itself having no known catalytic activity, interacts with non-acetylated tails of histone H2B, linking the protein with gene/chromatin regulation (Benvenuto et al., 2002). DET1 also interacts with a second *CONSTITUTIVE PHOTOMORPHOGENESIS 10* (COP10) which is a non-

cannonical E2 ubiquitin conjugating enzyme (Yanagawa et al., 2004) yet lacks enzymatic activity, and a gene involved in the DNA damage response, *DAMAGED DNA BINDING PROTEIN 1* (DDB1) (Schroeder et al., 2002). This tripartite (CDD) complex in turn can interact with a *CULLIN 4* (CUL4) and RBX1 to form a functional E3 ubiquitin ligase complex (Chen et al., 2006). However, the functional significance of this larger complex is not completely understood. The CDD complex functions as a transcriptional co-repressor that is recruited by two circadian-clock associated transcriptional repressors, *LATE ELONGATED HYPOCOTYL* (LHY) and *CIRCADIAN CLOCK ASSOCIATED 1* (CCA1) (Lau et al., 2011). Yet, despite the vast wealth of information gained within the past two decades since DET1 was first described, no single model has been able to sufficiently explain the numerous phenotypic changes associated with its loss-of-function.

Histone modification and DNA methylation are often acted upon as part of gene regulatory programs (Li et al., 2007; Bannister and Kouzarides, 2011; He et al., 2011). In plants, a combination of DNA methylation of all three sequence contexts (CG, CHG and CHH where H=A,C,T) is often associated with non-transcribed genomic regions, especially transposons or repetitive regions (Zhang et al., 2006; Lister et al., 2008). Previous reports suggest an association between histone acetylation (through HDA6) and DNA methylation (Probst et al., 2004), and it has been suggested that histone modification and DNA methylation may form a positive feed-forward loop which can strengthen heterochromatin formation at silenced loci (He et al., 2011). Other groups have suggested that light regulation of gene expression may involve histone modification, as genes regulated by light show similar fluctuations in activating or repressive histone modifications (Guo et al., 2008). Additionally, a histone acetyltransferase, GCN5, has a mild long-hypocotyl phenotype, indicative of attenuated

photomorphogenesis (Benhamed et al., 2006). However, specific regulatory points linking light signaling and histone modification have not been demonstrated.

Given the overwhelming changes in gene expression caused by lesions in the *det1* mutants, the pleiotropic nature of the mutant phenotypes, and the possible DET1 complex interaction with chromatin, we set out to address the role of *DET1* in chromatin stability by using a genome-wide approach to study the methylome of *det1*.

Results and Discussion

Whole-genome tiling arrays reveals methylation defects in *det1-1* mutant plants.

To determine whether DET1 has a role in chromatin maintenance or remodeling, we obtained and analyzed data from a 5-methylcytosine immunoprecipitation (mCIP) experiment previously performed (Chen, Gregory, Ecker, and Chory, unpublished data). A total of eight whole-genome tiling arrays were analyzed, containing bound and unbound (non-precipitated) DNA following mCIP from 5-day old etiolated wild-type (WT, Col-0) and *det1-1* seedlings. Methylated regions were identified as genomic regions from these arrays using TileMap software to call peaks (Ji and Wong, 2005). Overall, when array data from bound fractions was compared to that from unbound fractions, 10,122 methylated regions were identified in dark-grown WT seedlings and 8,603 methylated regions were identified in dark-grown *det1-1* seedlings (Figure 1-1). When these two data sets were compared, 4,697 of the methylated regions in Col-0 were unique (non-overlapping with methylated regions in *det1-1*) and only 2,004 methylated regions were unique in *det1-1*. When the Col-0 bound fraction data were compared directly to the *det1-1* bound fraction (a much more stringent analysis), a total of 297 regions were identified as hypomethylated in *det1-1*, compared to just 54 hypermethylated regions. Many demethylation events occurred among the euchromatic

arms of each chromosome, though centromeric methylation was also affected in *det1-1* (Figure 1-1). Overall, from the bound vs. unbound analysis, over 10% of genomic DNA was found to be demethylated in *det1-1*. To validate the tiling array data, we selected 12 regions predicted to be differentially methylated, and sequenced these regions following sodium bisulfite conversion of DNA extracted from 5-day old *det1-1* and Col-0 etiolated seedlings. Sodium bisulfite treatment of non-methylated cytosines converts them into uracil residues, which read as thymidine residues when PCR-amplified, cloned, and sequenced. 5-methylation protects cytosine residues from conversion, allowing for facile identification of methylated cytosines. Of these nine regions, eight were predicted by tiling array analysis to be hypomethylated, and one region hypermethylated. Eight of the predicted changes were confirmed by bisulfite sequencing, although one region contained an opposite methylation state (Figure 1-2). Thus, while we could confirm the majority of cases, artifacts associated with tiling array analysis (not least of which the imprecise definition of methylated cytosine residues) may be the confounding agent in those regions that we could not validate.

Little significant overlap exists between de-methylated regions in *det1-1* and light-regulated gene expression

When coding genes affected in DNA methylation were examined, no significant preference for a particular genic region was observed, nor did any functional annotation appear to be enriched following GO analysis (Figure 1-1). However, several genes within the RPP5 R-gene cluster were significantly demethylated (Figure 1-1), which correlated with a significant up-regulation of mRNA. This may be partially causative of the dwarf phenotype of *det1-1*, as overexpression of defense-related components (e.g. the BAL gene) can substantially reduce plant stature (Stokes et al., 2002). We re-

examined previously published microarray data from dark- and light-grown wild-type and *det1-1* seedlings (Schroeder et al., 2002), and compared differentially regulated genes to the differentially methylated regions identified by our tiling array analysis. We classified light-regulated genes in wild-type and *det1-1* into six different categories: genes up- or down-regulated by light in wild-type, but not differentially expressed in *det1-1*, genes up- or down-regulated by light in *det1-1* but not differentially expressed in wild-type, and genes oppositely regulated by light in *det1-1* when compared to wild-type (Figure 1-4). Five of the six gene classes showed substantially less methylated regions (as measured by the cumulative length of methylated regions in basepairs divided by the number of genes within each category). Only one gene class (genes down-regulated by light in wild-type, but up-regulated by light in *det1-1*) showed comparable levels of methylation, however these genes were very few compared to the other classes, and insufficient data may exist to make major conclusions about methylation and genes within this class. Overall, we did not see an overwhelming preference for DNA demethylation in *det1-1* for any particular type of light-regulated gene, and speculate that whatever function DET1 may have in maintaining or introducing DNA methylation, it is not specific to light-regulated genes in the dark.

5-aza-2'-deoxycytidine treatment is insufficient to drive de-etiolation in the dark

To test the causality of DNA demethylation over de-etiolation, we utilized a drug, 5-aza-2'-deoxycytidine (5-AdC), a cytosine analog, which cannot be methylated. Thus, when this nucleotide is introduced into genomic DNA, it should mimic a demethylation event. If DNA demethylation is sufficient to trigger the aberrant etiolation phenotype in *det1-1*, when wild-type seedlings are treated with 5-AdC, de-etiolation phenotypes should be apparent in the absence of light. When these seedlings were grown for 5

days on increasing doses of 5-AdC in dark conditions, no signficant change in etiolation was apparent apart from a decrease in hypocotyl length and inhibition of root elongation, even when very high (and possibly toxic) doses of the drug were applied (Figure 1-5). From this experiment alone, we cannot exclude the possibility that a specific 5-AdC incorporation event is necessary to drive de-etiolation, or even whether in the dark (when cells are mostly elongating, not dividing (Gendreau et al., 1997) that any incorporation at all would occur. It is possible that we did not screen enough seedlings (as the demethylation incurred by 5-AdC treatment would be stochastic), or that developing embryos would need to be treated. However, absent these experiments giving a positive result, we cannot conclude that the overall demethylation events observed in *det1-1* is a direct cause of the phenotypes observed, or a mere consequence of such changes across the entire transcriptome.

Conclusions

Despite convincing evidence demonstrating cytosine methylation defects in the *det1-1* mutant, neither the mechanism by which this occurs, nor the functional relevance of loss of DNA methylation is currently understood. Recently, the DET1 complex has been implicated in nucleotide excision repair, which is one possible method (along with base-excision repair, or BER) by which methyl-cytosine residues are removed from chromatin (Gehring et al., 2009; Castells et al., 2011). It would be interesting to study whether demethylation in *det1-1* mutants is due to defects in NER, BER, or both (although the necessity for DET1 during NER in plants would argue against this) (Castells et al., 2011). Aberrant DNA methylation in *det1-1* mutants could also be due to its role as a transcriptional co-repressor (Lau et al., 2011), although this transcriptional mediation has not been conclusively linked to any change in chromatin, degradation of

transcriptional or chromatin modifying component, or even direct inhibition of transcriptional activity. It is tempting to speculate that DET1 is acting either directly on chromatin as suggested by Benvenuto et al. (2002) or is acting through degradation of a chromatin-decompressing enzyme, e.g. GCN5 or a DNA methyltransferase. However, it remains to be shown whether the transcriptional co-repression activity of DET1 requires interaction with the CUL4/RBX1 E3 ubiquitin ligase complex, which would implicate proteosomal degradation as an essential component of DET1 function. Lastly, as DNA methylation is heritable, it would be very interesting to study whether the DNA methylation defects in *det1-1* are exacerbated by many generations of propagation, and whether the *det1-1* methylome is transgenerationally stable.

Materials and Methods

Tiling array analysis

Hybridization data from whole-genome *Arabidopsis thaliana* tiling arrays derived from bound and unbound fractions following 5-methylcytosine immunoprecipition of Col-0 and *det1-1* genomic DNA were analyzed using the TileMap software described previously (Ji and Wong, 2005) using a posterior probability p=0.5. BED files generated from this analysis were compared in two ways: bound vs. unbound fractions (for *det1-1* and Col-0 separately), or bound (*det1-1*) vs. bound (Col-0) directly. Hyper- and hypomethylated regions were determined from an overlap comparison using the bound vs. unbound data set. Candidate regions were selected based off this analysis for bisulfite sequencing.

Microarray analysis

Previously published from Affymetrix 8k microarray data (Schroeder et al., 2002)

was processed using the RankProduct software tool (Hong et al., 2006). Genes with log2-transformed fold changes greater than two were classified as differentially expressed, while fold changes less than two were classified as not differentially expressed. Genomic positions of differentially expressed genes were determined based on the TAIR9 genome release, and compared with differentially methylated regions determined by tiling array analysis.

Bisulfite sequencing

Genomic DNA from 5-day old dark-grown *det1-1* and Col-0 seedlings was extracted using the DNEasy Plant DNA Extraction Kit (Qiagen, Valencia, CA USA) according to the manufacturer's instructions. Genomic DNA was then sonicated at 4°C for 5 cycles of 30 second pulses followed by 2 minutes cooling. The sonicated DNA was then subjected to bisulfite sequencing using the Bislufite Conversion Kit (Qiagen, Valencia, CA USA), according to the manufacturer's instructions. Degenerate primers (listed in table 1-1) designed to amplify regions of differential methylation were then used in a polymerase chain reaction (for 35 cycles) using a PfuTurbo Cx DNA polymerase (Stragene, Santa Clara, CA USA), designed to read through uracil incorporation. Amplified DNA was then gel-purified using the QiaQuick Gel Purification Kit (Qiagen, Valencia, CA USA), and ligated into a TOPO Zero Blunt II vector (Invitrogen, Carlsbad, CA USA) via blunt-end ligation, according to the manufacturer's instructions. Ligated plasmid DNA was then transformed into DH5alpha *E. coli* cells, and up to 20 colonies were selected for plasmid isolation and DNA sequencing.

Plant growth conditions

Wild-type (Col-0) and *det1-1* mutant seedlings were grown on ½ MS + 2% agar

plates at high density for up to 5 days in dark conditions. For 5-aza-2'-deoxycytidine experiments, an appropriate amount of the drug (Sigma, St. Louis, MO) was added to the growth medium, and seedlings were grown under dark or continuous white light conditions for 5 days at 22ºC.

Acknowledgements

We would like to acknowledge Dr. Kunha Chen, Dr. Brian Gregory, and Dr. Joseph Ecker for generously allowing us to use their *det1-1* mCIP tiling array data. Portions of Chapter 1 are taken from a study which was conducted by Chen, Kunhua; Cole, B.; Gregory, Brian; Ecker, Joeseph; and Chory, Joanne, 2007. We would also like to thank Dr. Chris Bowler for discussion of DET1 function. This work was funded in part by an NSF IGERT grant (to B.C.).

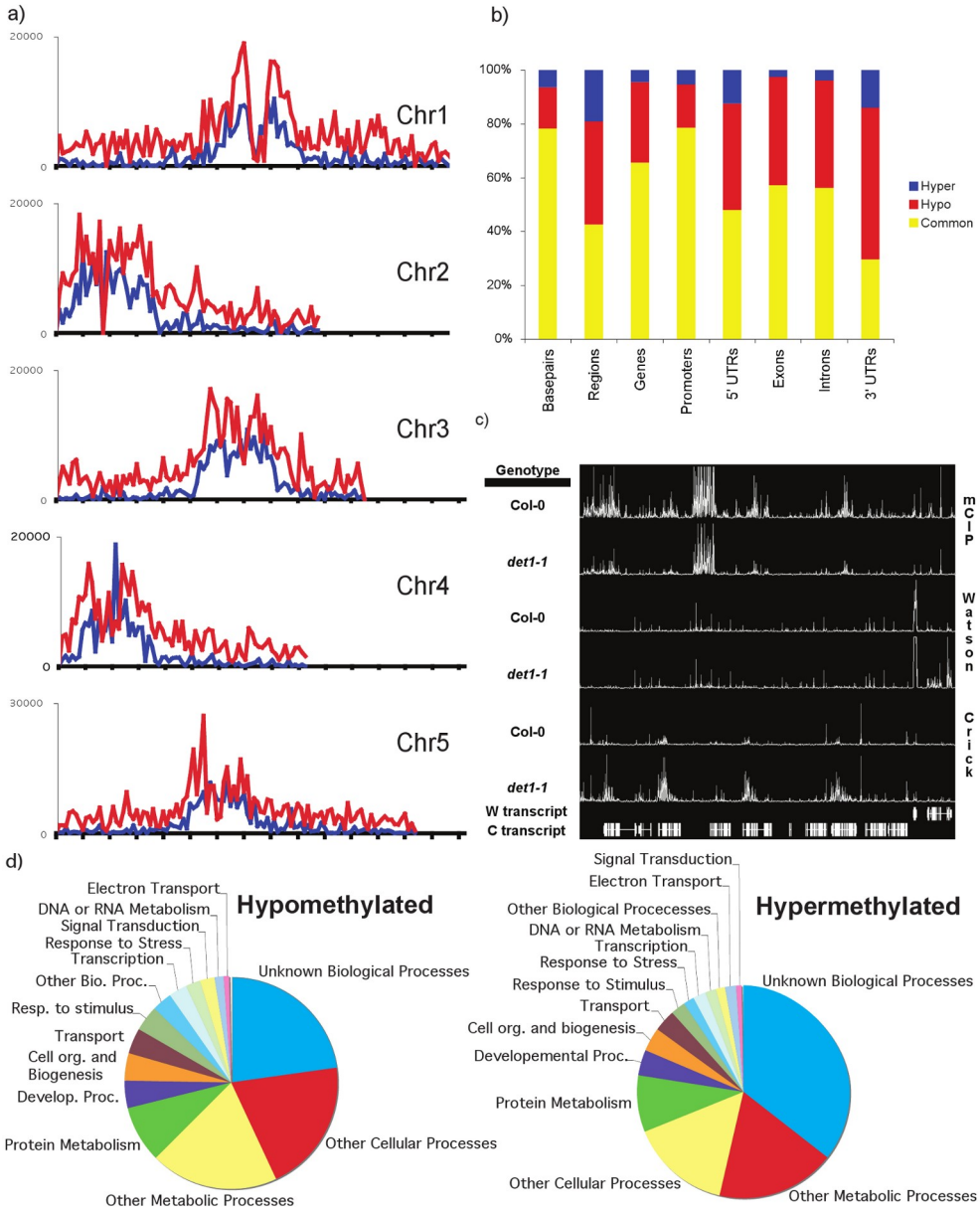

Figure 1-1: Genome-wide DNA demethylation is evident in *det1-1* via whole-genome tiling array analysis. a) Hypermethylated (blue) and hypomethylated (red) regions from overlapping and non-overlapping regions detected when bound and unbound fractions from *det1-1* and Col-0 tiling arrays are compared. Total region length (in basepairs) was combined into 0.25 Mbp bins, and plotted as a function of chromosomal position. b) total % hypermethylated (blue) hypomethylated (red), and unchanged methylation (yellow) occuring within various gene components, when *det1-1* and Col-0 are compared as in a). c) One genomic region (the RPP5 cluster) which is hypomethylated in *det1-1*. 5-methylcytosine immunoprecipitation (mCIP) data, mRNA accumulation (on either Watson or Crick strands) and the associated gene models are plotted against chromosomal position. d) GO functional annotation for hyper- or hypomethylated regions in *det1-1*. Values were calculated by #genes within each category which were differentially methylated, as indicated.

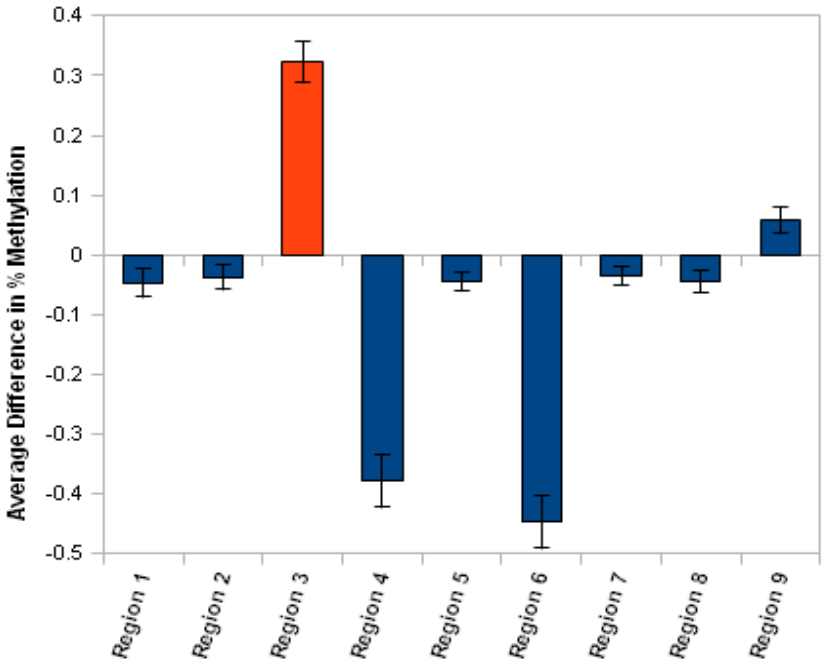

Figure 1-2: Bisulfite-sequencing validation of whole-genome tiling array analysis. Each region was identified as either hypermethylated (red bars) or hypomethylated (blue bars) by comparing bound and unbound fractions in *det1-1* vs. Col-0 seedlings. Average %methylated values for each cytosine residue contained in the region was calculated for *det1-1* and Col-0. For each cytosine residue, the Col-0 average was subtracted from the *det1-1*, and the average of these values was plotted for each region. Error bars represent ±s.e.m. for this average value.

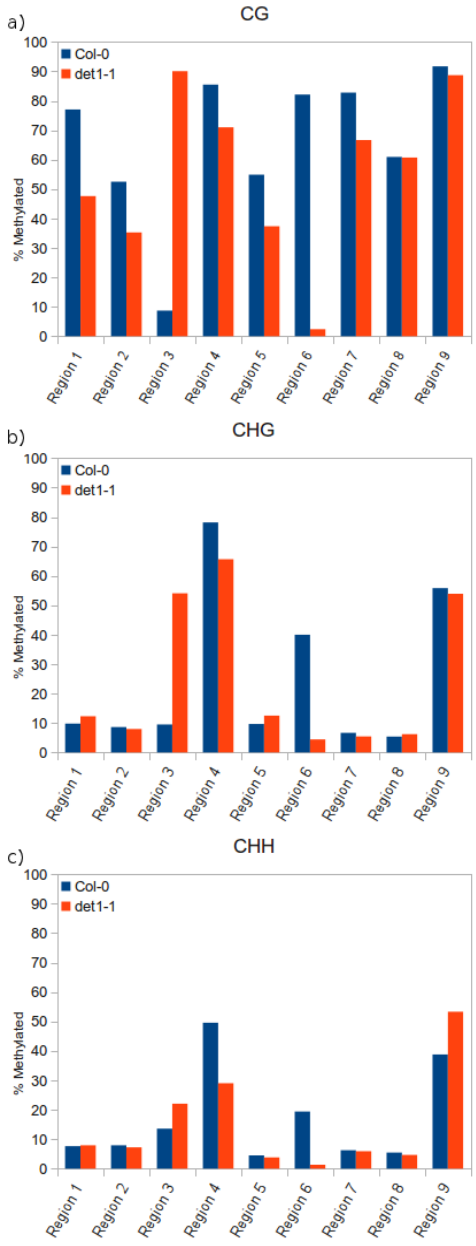

Figure 1-3: Context-specific methylation from bisulfite-sequencing data. Percent a) CG, b) CHG, and c) CHH (where H represents A, C, or T) methylation was calculated from Col-0 (blue) and *det1-1* (red) sequencing data for each of the regions described in Figure 1-2.

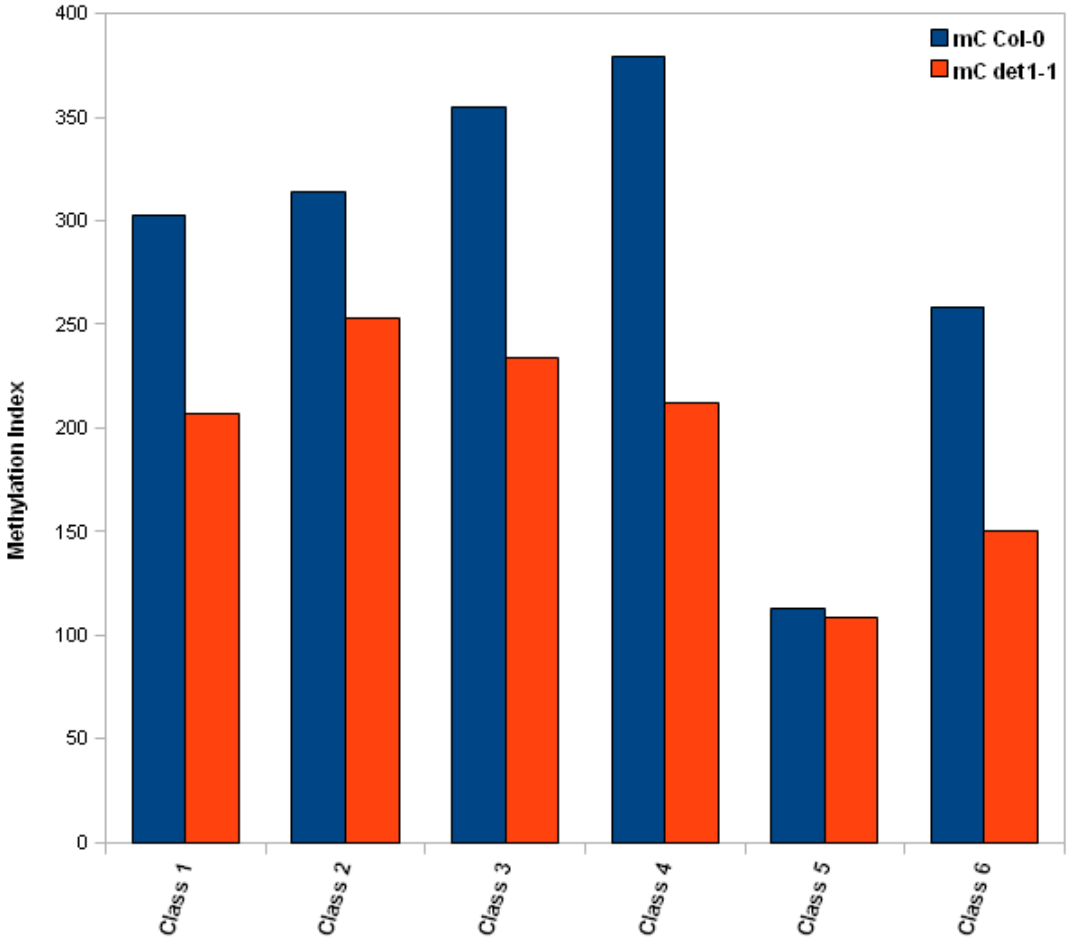

Figure 1-4: Differential methylation of light-regulated genes. Genes differentially regulated by light from a previous microarray analysis (Schroeder et al., 2002) were examined for their methylation profiles in *det1-1* and Col-0 seedlings. These genes were classified into six groups: genes up- or down-regulated by light in Col-0, but static in *det1-1* (Class 1 and 2, comprised of 339 and 350 genes, respectively), genes up-regulated by light in both Col-0 and *det1-1* (Class 3; 157 genes), genes up-regulated by light in Col-0 and down-regulated by light in *det1-1* (Class 4; 45 genes), genes down-regulated by light in Col-0 but up-regulated by light in *det1-1* (Class 5; 17 genes), and genes down-regulated by light in both Col-0 and *det1-1* (Class 6; 102 genes). A log2 fold change of 2.0 was used as a cutoff for up- or down-regulation. The methylation index is calculated as the sum of the length of methylated regions contained within each class of genes, divided by the number of genes in that class for *det1-1* (red) and Col-0 (blue).

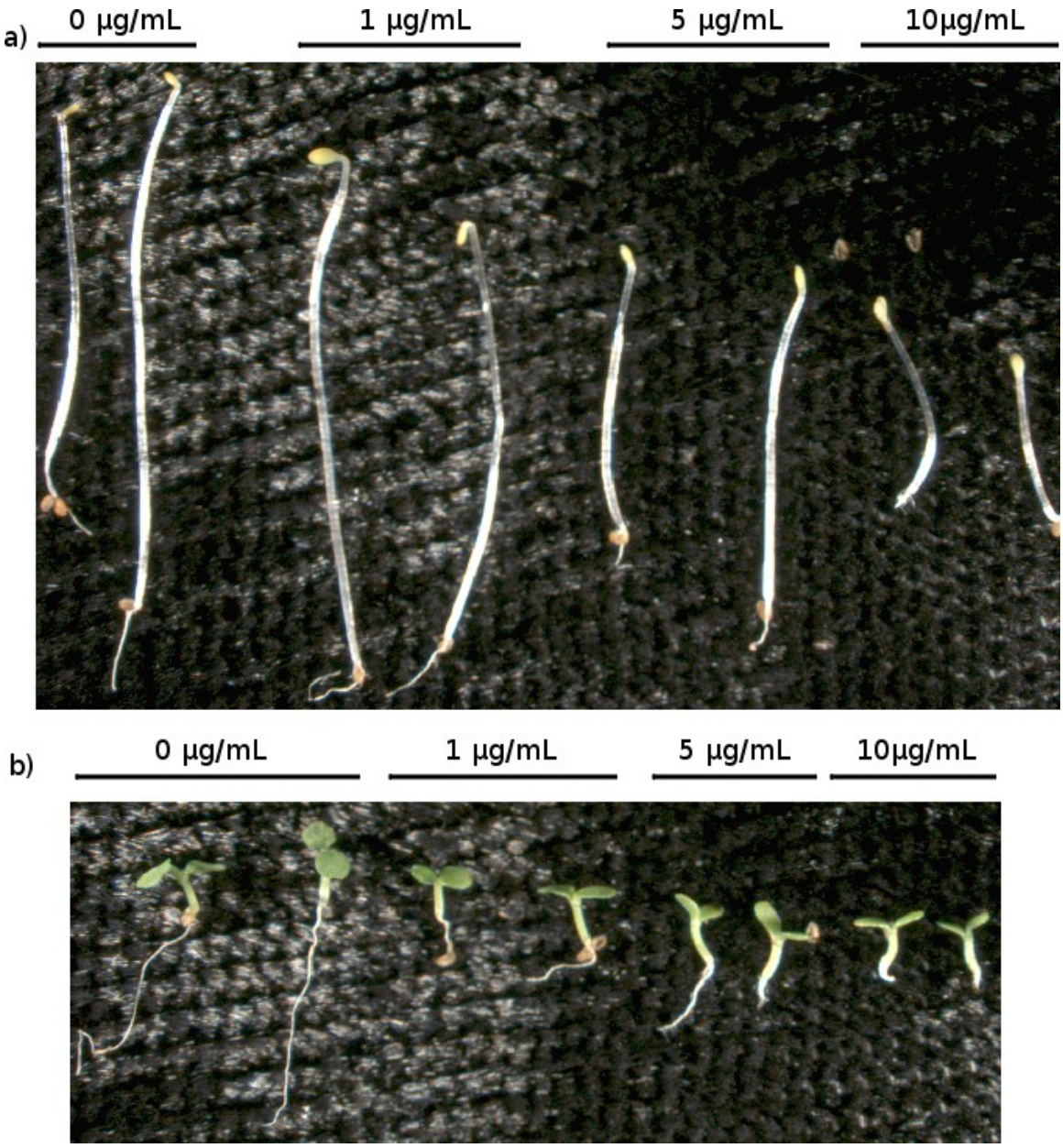

Figure 1-5: 5-AdC treatment does not significantly incur a de-etiolation phenotype in dark conditions. Col-0 seedlings were grown in a) darkness or b) fluorescent white-light conditions for 5 days on ½ LS agar plates supplemented with various concentrations of 5-aza-2'-deoxycytidine (as indicated). Besides a hypocotyl (and root shortening) phenotype, no significant de-etiolation phenotype could be observed under these conditions.

Table 1-1: Primers used for bisulfite-sequencing genomic DNA from *det1-1* and Col-0 seedling extracts. Chromosomal (Chr) locations are given, along with the sequenced length of each amplicon. Region numbers correspond to those indicated in Figure 1-2. Degenerate nucleotide base names follows IUPAC naming conventions (i.e. "R" represents any purine, "Y" represents any pyrimidine).

Region	Chr	Start Pos.	Length	Forward / Reverse Primer Sequence
Region 1	1	5185808	263	TATGGTYGYAGTGAGGYGTTT / RCTTTCTCAATAAAARTCARTCTATA
Region 2	1	2314576	359	GGYGATGAATYAGAGYAGGTT / ACAARCTATATCAATAAATAATCATAA
Region 3	1	19967297	423	TTGAYGGYAGTATAGTTAATAYGTT / RCCATTTTRCCTCTTTAATARTCA
Region 4	3	14783685	380	AGAAATTTGGAGATGAAGAYGTT / CAACTCATCAAATATCATRTCAAAA
Region 5	1	7174960	356	YTGATTTTTATGATTYYGATGGTTT / RCAAAAARCACCTTCATATCCAA
Region 6	5	14106471	331	GTTTTTAYAGTTGGATGGAGTTT / CCATTAATTCCTTCTCACCAA
Region 7	2	8149905	463	GAYTGTAAATAAGYGGGTTAGTT / AATCRCATTTATRACACTTCCAAAA
Region 8	5	4057895	499	GAYTGGAYTGAATGTTTATTTGTAT / RACTCAACTAAATATTRCTTCCAAA
Region 9	2	5212295	479	TAAAGTGATGGYTGAGTTATGTT / RCTACTAATATAACCAACAATTTAA

CHAPTER 2

Automated analysis of hypocotyl growth dynamics during shade avoidance in Arabidopsis

Benjamin Cole, Steve A. Kay, Joanne Chory

Abstract

Plants that are adapted to environments where light is abundant are especially sensitive to competition for light from neighboring vegetation. As a result, these plants initiate a series of changes known as the shade avoidance syndrome, during which plants elongate their stems and petioles at the expense of leaf development. Although the developmental outcomes of exposure to prolonged shade are known, the signaling dynamics during the initial exposure of seedlings to shade is less well studied. Here, we report the development of a new software-based tool, called HyDE (Hypocotyl Determining Engine) to measure hypocotyl lengths of time-resolved image stacks of Arabidopsis wild-type and mutant seedlings. We show that Arabidopsis grows rapidly in response to the shade stimulus, with measurable growth after just 45 min shade exposure. Similar to other mustard species, this growth response occurs in multiple distinct phases, including two phases of rapid growth and one phase of slower growth. Using mutants affected in shade avoidance phenotypes, we demonstrate that most of this early growth requires new auxin biosynthesis via the indole-3-pyruvate pathway. When activity of this pathway is reduced, the first phase of elongation growth is absent, and this is correlated with reduced activity of auxin-regulated genes. Finally, we show

that varying shade intensity and duration can affect the shape and magnitude of the growth response, indicating a broad range of the elongation response to shade.

Introduction

Plants need light to survive and are often in competition with other plants for photosynthetically active wavelengths of light (Franklin and Quail, 2010). As such, plants have evolved sophisticated photoreceptors that are capable of sensing the presence of neighbors by monitoring the ratio of red light (R) (which chlorophyll absorbs as part of the photosynthetically active light spectrum) to far-red light (FR) (which chlorophyll does not absorb, and which is thus reflected and transmitted through leaves) (Kasperbauer, 1987; Ballaré et al., 1990). A high R/FR ratio indicates a sparsely populated environment and an abundance of photosynthetically active radiation. Conversely, a low R/FR ratio (<1) indicates the presence of nearby vegetative neighbors that may soon compete for available light. This low R/FR ratio initiates a suite of responses, termed the shade avoidance syndrome (SAS), that are of physiological and agricultural importance. The SAS has been extensively studied in the reference plant *Arabidopsis thaliana* (Smith and Whitelam, 1997; Franklin, 2008). Plants grown under shade have a decreased germination rate, increased hypocotyl and petiole elongation, inhibition of both leaf expansion and root elongation, reduced chlorophyll content, a tendency to flower early, reduced fecundity, and an increased susceptibility to herbivory (Smith and Whitelam, 1997; Izaguirre et al., 2006).

The Arabidopsis hypocotyl is an excellent model for studying shade phenotypes due to its simple structure, sensitivity to light, small cell number (approximately 20 cells in each cell file), and reliance on cell expansion versus cell division for elongation growth (Gendreau et al., 1997; Chen et al., 2004). Seedlings that are foraging for light have long

hypocotyls, while those growing under bright light (R/FR > 1) have shorter hypocotyls. Hypocotyl length is inversely proportional to the fluence rate of white light. End-point assays quantifying shade avoidance phenotypes are typically performed by measuring hypocotyl length after several days of growth in light supplemented with far-red radiation (Salter et al., 2003; Sessa et al., 2005; Lorrain et al., 2008). Various studies under these conditions have enabled development of a tentative model whereby the photoreceptors phytochromes B, D and E, perceive the shift in the ratio of R/FR light (Child and Smith, 1987; Smith, 2000). This allows accumulation of at least two phytochrome-interacting basic helix-loop-helix (bHLH) transcription factors, PIF4 (*PHYTOCHROME INTERACTING FACTOR 4*) and PIF5 (Huq and Quail, 2002; Khanna et al., 2004; Lorrain et al., 2008), which promote growth by modulating gene expression (Lorrain et al., 2008). Of the three phytochromes in the pathway, phyB has the strongest role, while phyD and phyE have relatively minor roles (Franklin et al., 2003). A third bHLH protein, HFR1 (*LONG HYPOCOTYL IN FAR-RED LIGHT*), whose transcript is rapidly induced upon exposure to shade, constitutes part of a negative feedback mechanism by binding to PIF4 and PIF5, and inhibiting their DNA-binding (and thus growth-promoting) activity (Fairchild et al., 2000; Duek and Fankhauser, 2003; Sessa et al., 2005; Hornitschek et al., 2009). Seedlings with mutations in the photoreceptor phyA showed exaggerated hypocotyl elongation upon transfer to shade after 2 days of growth in continuous white light (Johnson et al., 1994), consistent with phyA signaling through HFR1 (Fairchild et al., 2000). However, the role of phyA in shade avoidance is unclear, as older seedlings do not display this phenotype (Z. Zheng and J. Chory, unpublished data).

Gene expression studies have implicated other transcription factors in mild hypocotyl-length phenotypes, including the bHLH-containing negative regulators PIL1 (encoded by *PHYTOCHROME INTERACTING FACTOR LIKE 1*), PAR1 and PAR2 (*PHY*

RAPIDLY REGULATED genes), as well as a positive regulator, ATHB-2 (encoded by *A. THALIANA HOMEODOMAIN BOX 2*), which is an HD-ZIP class protein (Schena et al., 1993; Carabelli et al., 1996; Steindler et al., 1999; Devlin et al., 2003; Salter et al., 2003; Sessa et al., 2005; Roig-Villanova et al., 2006), but their immediate targets have not been characterized.

New auxin biosynthesis is necessary for shade-induced hypocotyl elongation, as indicated by the discovery of an auxin biosynthesis gene, *SHADE AVOIDANCE 3* (*SAV3*), which encodes the tryptophan aminotransferase TAA1 (*TRYPTOPHAN AMINOTRANSFERASE OF ARABIDOPSIS 1*), which converts tryptophan to indole-3-pyruvic acid. Exposure to shade induces auxin biosynthesis in wild-type plants (producing up to 50% more auxin within 1 h), but not in plants lacking functional SAV3, in which shade avoidance phenotypes are severely reduced (Stepanova et al., 2008; Tao et al., 2008). Treatment with NPA (1-naphthylphylamic acid), a polar auxin transport inhibitor, also attenuates shade-induced hypocotyl elongation (Steindler et al., 1999). Polar auxin transport has thus been shown to mobilize auxin from the leaves to sink tissues, such as the hypocotyl and petiole, consistent with preferential expression of SAV3 in leaf tissue (Tao et al., 2008). Finally, gibberellic acid (GA) promotes the shade response by inducing degradation of DELLA-containing proteins (a five-member family of growth repressors) that can bind to and inhibit PIF transcription factors (Djakovic-Petrovic et al., 2007; de Lucas et al., 2008; Feng et al., 2008). Thus, the shade avoidance response provides an informative platform to study the intersection of light and various hormone signaling pathways as they relate to plant physiology, growth regulation and environmental adaptation (Vandenbussche et al., 2005; Jaillais and Chory, 2010).

Although some of the components that drive the shade avoidance response have

been identified, a gap remains between the time at which physiological phenotypes (several days after exposure) and molecular events (usually within 1–4 h) are studied. Physical methods have been used to quantify growth in *Vigna sinensis* epicotyls (García-Martínez et al., 1987) and Sinapis alba stems (Morgan et al., 1980; Child and Smith, 1987; Casal and Smith, 1989), and have shown that a rapid multi-phasic growth response can occur upon exposure to shade. Similar physical techniques have been used to study etiolated growth in Arabidopsis seedlings undergoing photomorphogenesis in response to monochromatic light (Parks and Spalding, 1999), and revealed subtle differences in growth patterns among photoreceptor mutants. While informative, these studies relied on invasive strategies to record elongation rates, which are difficult (but not impossible) to perform on delicate and morphometrically dynamic Arabidopsis seedlings (Folta and Spalding, 2001; Miller et al., 2007), for which a wealth of experimental tools exist. Recently, non-invasive imaging and feature-detection technologies have enabled the study of real-time growth dynamics in etiolated seedlings (Miller et al., 2007; Wang et al., 2008, 2009), representing a great improvement over previous methods. However, automated image analysis of dark-grown seedlings is different from that of light-grown seedlings, as light-grown petioles can grow independently of the hypocotyl, and existing software exploits features of the petiole/cotyledon junction to analyze dark-grown seedlings (Wang et al., 2009). Thus, new imaging approaches are required for imaging of light-grown seedlings.

Our goal was to assess hypocotyl elongation over short time scales by developing an image-based phenotyping platform. Here, we describe HyDE (Hypocotyl Determining Engine), a new software tool for quantifying hypocotyl length on time-resolved image stacks of single light-grown seedlings. We used this tool to reveal multi-phasic growth patterns of Arabidopsis seedlings in response to shade, and to study the

short-term effect of mutations in the shade avoidance response pathway. We defined distinct periods of hypocotyl elongation after exposure to shade, and correlated these periods with accumulation of mRNA for known shade marker genes. Finally, we showed that the magnitude and shape of the shade response could be dynamically altered by adjusting the light regime. As such, our results provide a kinetic framework to further characterize early events and identify novel components of the shade avoidance perception and response pathways.

Results and Discussion

HyDE software can image light-grown hypocotyl dynamics in an automated assay

To establish correlations between shade-regulated molecular events and the phenotypes they are thought to control, we developed an assay that is capable of measuring physiological phenotypes over the same short time scales used to study molecular phenotypes. Our new assay adapts the Phytomorph CCD-camera based imaging system developed by Miller et al. (2007) to image light-grown Arabidopsis hypocotyls in a three-channel LED chamber, simulating high- and low-R/FR light conditions (Figure 2-1). To avoid interference from the far-red light used to simulate shade, we utilized an IR filter with a cut-off at 790 nm, slightly longer than used previously (720 nm), but still able to detect the 880 nm backlight source (Miller et al., 2007). To accompany the imaging set-up, we devised a software tool, HyDE, to automatically measure the length of hypocotyls in a time-resolved image series. The software (whose algorithm is diagrammed in Figure 2-1) first converts a cropped raw seedling image to a binary (foreground/background) format, and calculates a Euclidean distance transform (EDT). It identifies local maxima within the EDT, indicating the centroid points of major organs (e.g. cotyledons and the shoot apical meristem). HyDE

then constructs a digital hypocotyl based on the center line of the imaged hypocotyl, using the bottom horizontal pixel slice as a reference to determine the horizontal position of the hypocotyl. The hypocotyl should be the only structure present on the lowest portion of the image. HyDE terminates the digital hypocotyl where it intersects with the first local maximum corresponding to the shoot apical meristem, which forms a bulge where the petioles initiate. This hypocotyl center line is then spline-smoothed, and its length is recorded for all images in the stack. Our method works best on young (4- to 7-day-old) seedlings, as they lack fully emerged true leaves, which can obscure morphological information at the hypocotyl–petiole junction. Although we have not tested our software on older seedlings, we expect that this 4–7 day window represents the most informative time to capture dynamic information, as older Arabidopsis hypocotyls are less responsive to growth stimuli. Similarly, selected seedlings that grew such that the cotyledons extended perpendicular (±15°) to the plane of imaging, so they would not interfere with hypocotyl length measurements. The software is available for download from http://cactus.salk.edu/hyde.html.

We tested the image-processing algorithm on 5-day-old long-day entrained (16 h fluorescent white light/8 h dark) wild-type Arabidopsis accession Columbia (Col-0) seedlings to assay for growth when released (at zeitgeber time ZT12) into continuous light conditions (LED-simulated daylight). Under these conditions, the hypocotyls of wild-type seedlings did not elongate during the majority of the subjective dark period, instead exhibiting a major growth peak during the middle of the day, beginning at ZT2 and ending at ZT12 (Figure 2-2). This is consistent with published circadian and diurnal growth data (Nozue et al., 2007). We conclude from these experiments that the HyDE software is capable of measuring hypocotyl length over very short time scales, being able to detect significant length differences over periods as short as 10 min, a resolution

that is useful for understanding the growth kinetics of shade avoidance responses.

Arabidopsis thaliana seedlings respond to shade within 1 h, exhibiting a multi-phasic growth pattern that varies with the R/FR ratio

To assay for hypocotyl-specific growth during the shade avoidance response, we manipulated the far-red light intensity to mimic the very earliest ‘shade’ conditions that plants encounter: the threat of shade (reflected FR light) from neighboring vegetation. Based on field studies of soybeans (Glycine max), which indicated that reductions in R/FR may be more prevalent at dusk (Kasperbauer, 1987), we decided to treat the seedlings towards the end of the subjective day under diurnal conditions. Five-day-old Arabidopsis seedlings (grown under fluorescent lights under long-day conditions) were transferred to the imaging platform at ZT12, under high R/FR conditions (R/FR = 2.37). The seedlings were imaged for 2 h to establish a baseline growth pattern, before being challenged with a marked increase in supplementary FR light, decreasing the R/FR ratio to 0.23. After the start of treatment, we imaged seedlings for a further 9.5 h, and hypocotyl lengths were measured using HyDE (Figure 2-3). Wild-type seedlings exhibited a lag period of about 45 min after exposure, growing at a basal rate of about 0.1 μm min−1, before rapidly elongating at a rate of 0.45 μm min−1 until approximately 150 min after exposure. The hypocotyl growth then slowed to a rate of 0.2 μm min−1, until about 230 min after exposure, when it accelerated to approximately 0.55 μm min−1 for the remainder of the experiment.

Based on the shape of the curve, we defined four phases of growth under shade: a lag phase (from approximately 30 min before exposure to 45 min after exposure), an initial growth phase (45–150 min after exposure), a slowdown phase (150–230 min after exposure), and a second growth phase (from 230 min after exposure to the end of the

assay). These phases are similar to those observed in *Sinapis alba* primary stems and first internodes (Morgan et al., 1980; Child and Smith, 1987; Casal and Smith, 1988); however, the observed lag time in Arabidopsis is significantly longer reported previously for Sinapis. Additionally, although *Sinapis alba* grows more quickly in the first phase than the second, Arabidopsis hypocotyls grew at a slightly faster rate during the second growth phase than the first. The results from cowpea (Vigna unguiculata) indicated rapid initiation of growth within 60 min after exposure to supplementary FR, with no reduction in the growth rate until 10 h after the start of the experiment (García-Martínez et al., 1987). These differences in kinetics may reflect the differences in species, tissues or experimental set-up.

To explore whether the severity of shade has a strong effect on growth kinetics, we treated wild-type seedlings as above, but decreased the R/FR to 0.65 (mild shade), 1.2 or 1.6 (non-shade), comparing growth curves from these seedlings to those that were not treated or had the R/FR lowered to 0.23 (full shade). The elongation response was very sensitive, with a measurable increase in the growth rate even during the two least intense treatments (R/FR = 1.6 and 1.2, values that were previously assumed to be at or above the threshold for eliciting a shade avoidance response) (Smith, 2000) (Figure 2-3). Mild shade treatment results in slower growth in both elongation phases (with that in phase IV being slower than that in phase II) when compared to that in full shade, in which seedlings grew faster in phase IV than in phase II (Figure 2-3). Overall, there was an inverse correlation between the severity of the shade treatment and the magnitude of the elongation responses. A slowdown period was observed for all treatments, during which seedlings treated with 0.23, 0.65 and 1.2 R/FR light grew at approximately the same rate (0.2 μm min−1), but those treated with 1.6 R/FR grew at a slower rate (approximately 0.09 μm min−1), suggesting that this slowdown period does not require a

certain amount of growth to occur in order to be observed. Our sensitive hypocotyl measurement method suggests that either the threshold R/FR ratio that elicits a shade response in Arabidopsis hypocotyls is higher than previously thought, or that plants are sensitive to the change in the ratio rather than the absolute ratio itself. For further experiments, we decided to use the most severe treatment (R/FR 0.23), as it yielded the most dramatic results.

The time of treatment has a minimal effect on the quality and magnitude of the response within an 8 h window

Although growth in the absence of shade treatment appeared to be negligible (Figures 2-2 and 2-4), we wished to assess whether treating seedlings at various times of the day would affect the magnitude or quality of the resulting growth curve. We subjected wild-type seedlings to the same pre-treatment conditions as before, but applied supplemental FR light 2, 4, or 6 h later than our other assays (at ZT16, ZT18 and ZT20, respectively; Figure 2-5). The quality of the growth response was nearly identical to that for seedlings treated at ZT14: the seedlings had a sharp initial increase in growth rate approximately 45 min after treatment, which slowed after approximately 150 min, followed by growth at a faster rate after approximately 230 min (Figure 2-5). The similarity of these responses is particularly apparent when the data are superimposed such that the subjective time of treatment is the same (0 min, Figure 2-5). Because we did not keep the length of shade exposure constant for each assay, we cannot say that growth during phase IV for the seedlings treated at ZT20 is identical to that exhibited by seedlings treated at ZT14, but we observed that the lag period (phase I) is identically timed, the slope and duration of the first growth phase (phase II) are similar, and that these seedlings have a similar slowdown at the same time (Figure 2-5). Thus, it appears

that, if the time of treatment has a strong gating role in regulating hypocotyl growth in the shade, it is not immediately apparent during the 10 h period for which seedlings were treated (at the end of the day), although we cannot rule out the possibility of long-term temporal effects occurring after 12 h of treatment. Our data suggest that factors that affect the qualitative parameters of the shade growth response (e.g. the slowing observed in phase III) are likely to be initiated by the shade treatment itself. Thus, we saw little role for the circadian clock in promoting growth of hypocotyls within our time frame, in contrast to previous studies in which a more prominent role for clock regulation was apparent (Salter et al., 2003). However, we did not perform a full-scale circadian clock assay to directly test this hypothesis, and so we cannot contradict previous reports suggesting a more prominent role for the clock (Salter et al., 2003).

Auxin is necessary for proper initiation of the elongation growth response, and, together with PIF4 and PIF5, regulates its magnitude

We next tested whether mutations of some of the shade avoidance pathway components would alter the quality or magnitude of the shade growth response. Previous studies that quantified hypocotyl responses to shade in plants deficient in phytochrome A suggested a negative role for this photoreceptor on shade-induced growth (Johnson et al., 1994). We thought that at least one if not all growth phases in a *phyA* mutant would show higher growth rates, and therefore we imaged null *phyA-211* seedlings (Nagatani et al., 1993) using our shade assay. As shown in Figure 2-6, *phyA-211* seedlings showed normal timing and magnitude of the initial elongation and slowdown phases. However, although phase IV is initiated at the same time as in wild-type, *phyA-211* seedlings do not reach the same final growth rate as wild-type seedlings, resulting in slightly shorter hypocotyls at the end of the experiment. This is inconsistent

with studies suggesting a negative effect of phyA action on the shade elongation response (Johnson et al., 1994). Instead, our conditions (using seedlings older than those used by Johnson et al., 1994) highlight the proposed role of phyA in enhancing the response to low R/FR manifested by reduced phyB Pfr (far-red light absorbing form) levels (Casal, 1996), as opposed to the role phyA plays in mediating the high-irradiance response during de-etiolation.

We observed a more dramatic effect in *sav3-2* seedlings, which did not respond at all during the first approximately 4 h of the shade response, lacking growth in both phases II and III (Figure 2-6). They did show a sharp increase in elongation rate towards the end of the assay at approximately the same time that wild-type seedlings began their second elongation phase; however, this growth rate was only approximately 30% of that seen in wild-type seedlings in the same time period. These results suggest that new auxin biosynthesis by the SAV3/TAA1 pathway plays an important qualitative role in initiating the elongation response, and a quantitative role in maintaining high rates of elongation growth after several hours of shade exposure. We also speculate that the lag time observed directly after treatment (phase I) could be due to biosynthesis and transport rates, as the site of auxin synthesis (the cotyledon margins) is distinct from the hypocotyl (Tao et al., 2008). Regulation of TAA1 expression alone cannot account for the phenotypes observed, as its transcript abundance tends to decrease upon exposure to shade (Tao et al., 2008). Recent results suggest that auxin transport in etiolated hypocotyls is linked to phytochrome activity (Nagashima et al., 2008; Wu et al., 2010); however, the mechanism by which light regulates auxin biosynthesis or transport remains unclear.

pif4pif5 double mutant seedlings (Fujimori et al., 2004; Lorrain et al., 2008) exhibited all growth phases at the proper time, but the magnitude of both growth phases

was slightly less than wild-type growth rates, and this defect was more pronounced for phase IV than phase II growth (Figure 2-6). This mild phenotype suggests that, although the PIF4 and PIF5 transcription factors have a quantitative role in modulating growth, they either act redundantly with other growth regulators, or transcription has only a minor role in mediating the early elongation response to shade.

Gene expression patterns of shade marker genes correlate with phases of growth

To assess whether gene transcription follows a similar multi-phasic pattern, we prepared cDNA from wild-type plants at time points of the imaging assay reflecting each growth phase (0 and 30 min for the pre- and post-induction lag phase, 60 and 120 min for the first elongation phase, 180 min for the slowdown phase, and 360 min for the second elongation growth phase). We performed quantitative real-time PCR assays for PIL1, HFR1, ATHB-2, and IAA29 (Figure 2-7) transcripts, which were previously shown to be strongly induced after 1 h of shade exposure (Steindler et al., 1999; Salter et al., 2003; Tao et al., 2008). As expected, PIL1 expression was highly induced by the 30 min time point, and continued to increase until at least 120 min after exposure to shade. We observed a marked decrease in expression level at the 180 min time point, and a strong increase of expression after 360 min, consistent with phases III and IV of our imaging assays (Figures 2-3 and 2-7). The same general pattern was observed for HFR1, although expression was merely maintained at a constant level through phase III compared to the expression peak during phase II, before increasing again towards the end of the assay (Figure 2-7). Although PIL1 and HFR1 have both been shown to be negative regulators of the shade growth phenotype (Salter et al., 2003; Sessa et al., 2005; Hornitschek et al., 2009), their expression patterns appeared to track growth. It is important to note that although expression levels fluctuated along the time course

consistently with growth rates, shade treatment increased RNA levels at all time points assayed.

We also measured the expression pattern of two genes related to auxin signaling, ATHB-2 and IAA29 (Carabelli et al., 1996; Steindler et al., 1999). The mRNA levels for each gene were induced quickly (ATHB-2 after 30 min, IAA29 after 60 min), and continued to be induced to the 120 min time point (phase II). However, both genes showed reduced expression during phase III, and were not re-induced during phase IV. This is consistent with auxin signaling playing a stronger role towards the beginning of the assay, as indicated by the stronger *sav3* phenotype during phase II than phase IV (Figure 2-6). We speculate that the delayed induction response of IAA29 occurs as a consequence rather than a cause of the auxin-induced growth that occurs during the first elongation phase.

Elongation growth is reversible for at least 3 h of shade treatment

To understand the extent of the elongation response that can be elicited by transient shade, we exposed plants to severe shade for 0.5, 3 or 6 h before returning them to high R/FR light conditions (Figure 2-8). Even though the shade treatment was reversed prior to the expected time of the initial response (phase II), seedlings still exhibited some elongation growth for at least 15 min before slowing their growth rate to phase I levels when exposed to just 30 min of low R/FR (Figure 2-8). A similar reversal was seen for the 3 h treatment, in which seedlings did not initiate the second phase of the growth response (phase IV), and instead slowed to phase I growth rates until the end of the experiment. Seedlings exposed to only 6 hours of shade began to deviate from seedlings exposed continuously approximately 1 hour after reversion to high R/FR conditions, when growth slowed to a level greater than the phase I growth rates,

indicating that some residual growth remains despite the light reversal. This does not appear to be a lag in reversal of growth, as the elevated rate persists for at least 3 h, whereas the seedlings treated for 0.5 or 3 h reverted to basal growth levels within 1 h after the R/FR was increased (Figure 2-8). This leads us to speculate that either a growth factor (perhaps auxin) remains at high levels after a longer duration of treatment, or that the cells have committed to an elongation program whereby low R/FR enhances but is not necessary for continued elevated growth rates.

Conclusions

In summary, using temporally resolved imaging assays, we have shown that shade-avoiding hypocotyls exhibit multiple phases of elongation growth, controlled by separate, but possibly integrated mechanisms, one of which is new auxin biosynthesis mediated by SAV3. This response is mounted for a range of R/FR ratios, and the memory of the treatment can be maintained if longer durations of shade are applied. The time of treatment did not have a prominent role in promoting or restricting growth under our shade conditions within a 10 h time frame. Rather, it is likely that the mechanism controlling the dynamic shape of the growth curve is initiated by the treatment itself. Investigation into whether the circadian clock has a strong role in controlling the shade avoidance response at various times of the day (e.g. subjective dawn) would be an interesting subject for future research. Initiating multiple layers of control of elongation in response to the shade stimulus may provide the plant with many decision points before commitment to a shade-avoiding lifestyle. An initial burst of growth in the right direction after perception of a transient shade signal may be just enough to enable the plant to continue to intercept an optimal amount of light for photosynthesis, in which case it need not resort to the detrimental responses seen in plants growing in continuous shade.

However, if the signal is more persistent, such shade avoidance growth may be the best strategy to provide a competitive advantage under a less ideal environment. It will be interesting to explore further the mechanisms that control each phase of growth and how a decision is made to commit to a shade-avoiding lifestyle.

Materials and Methods

Plant growth and light conditions

Arabidopsis thaliana seeds were ethanol-sterilized and suspended in 0.1% agar for stratification prior to plating onto half-strength Linsmaier and Skoog (LS) 0.8% agar plates buffered with MES at pH 5.7. Plates were poured using a plastic mold that occluded half of a circular Petri dish, and the stratified seeds were plated on the ledge formed at the interface between the agar and the mold (such that the apical portions of the seedling grow unobstructed in air, while the basal tissues grow into the agar plate). Plates were grown under 16 h/8 h day/night cycles in growth chambers (Percival Scientific, http://www.percival-scientific.com/) supplemented with fluorescent and incandescent light [approximately 37 μmol m^{-2} sec^{-1} blue light (400–600 nm), approximately 30 μmol m^{-2} sec^{-1} red light (600–700 nm) and approximately 11 μmol m^{-2} sec^{-1} far-red light] for 5 days before being transferred to the imaging platform under LED light [approximately 37 μmol m^{-2} sec^{-1} blue light (400–600 nm), approximately 30 μmol m^{-2} sec^{-1} red light (600–700 nm) and approximately 11 μmol m^{-2} sec^{-1} far-red light] at ZT12 on the 5th day. Plants were then exposed to supplemental FR light by increasing the FR light intensity to reduce the R/FR ratio as indicated in each experiment. For RNA experiments, seedlings were grown on Whatman filter paper on top of half-strength LS agar (0.8%) plates under the same light conditions as for the imaging experiments.

Imaging platform

The imaging machinery consisted of two CCD cameras, one Marlin and one Guppy (Allied Vision Technologies, http://www.alliedvisiontec.com/), coupled to macro video zoom lenses (Edmund Optics, NT54-363 for the Guppy, http://www.edmundoptics.com/, Qioptics MVZL for the Marlin, http://www.qioptiq.com/) mounted to a rail on a thick aluminum surface (custom-built). Plates are held in sample mounts for circular or square Petri dishes, tightened by a thumb screw. The lenses were fitted with IR long-pass cut filters (NT54-755, Edmund Optics), which allow only wavelengths longer than 790 nm through. Seedling samples were back-lit with an IR LED back-light emitting at 880 nm (Edmund Optics). Image acquisition was achieved via a FireWire connection to a laptop computer, using AVT SmartView software (Allied Vision Technologies). This software allows imaging up to 15 frames per second for any duration of time; however, in the interest of saving disk space and maximizing the number of genotypes and conditions sampled, we saved images every 5 min (every 240th frame with a frame rate of 0.8 frames per second). Image stacks were cropped using ImageJ (http://rsbweb.nih.gov/ij/) after image acquisition but prior to processing with HyDE software, such that only one seedling hypocotyl was visible (and the hypocotyl was cropped from the very base of the image to avoid interference with the seed coat and agar surface). The imaging platform and analysis software are shown in Figure 2-1.

HyDE algorithm

The HyDE input consisted of the cropped image stacks as described above, and were converted to binary image format using the matlab image processing toolbox (http://www.mathworks.com/), which automatically determined the threshold grayscale

intensity value to assign foreground and background pixels. A coarse midline of the hypocotyl was determined by calculating the midpoint between two boundary pixels in successive horizontal pixel slices, ordered by the vertical position in the image. Large deviations between the current and previous horizontal slices (which typically occur within the petiole/cotyleon junction) was used by the algorithm to define a coarse upper boundary below which to look for the termination point of the hypocotyl. The coarse hypocotyl midline was then refined by finding the maximum Euclidean distance transform value (calculated using the MATLAB image processing toolbox) on these bounded midline points, and terminating the hypocotyl at that point (which should correspond to the hypocotyl/petiole junction). The hypocotyl midline was then smoothed using a 4th-order spline (utilizing three segments), and the distance was measured by summation of 0.1 pixel size increments along the length of the spline. This process was repeated for each image in the stack, and data from images that deviated by more than a defined number of pixels from the previous image were automatically rejected. Whole image stacks were removed from analysis if more than 10 consecutive images were rejected.

RNA extraction and quantitative real-time PCR

Seedlings grown under the indicated conditions were frozen in liquid nitrogen. Three biological replicates were collected per plate, approximately 10 seedlings per replicate. RNA was extracted from each seedling pool using an RNeasy plant mini kit (Qiagen, http://www.qiagen.com/) according to the manufacturer's instructions. cDNA was synthesized from 2 µg RNA using a Maxima cDNA synthesis kit (Fermentas, http://www.fermentas.com/) according to the manufacturer's instructions. Ten microliters of each 100-fold diluted cDNA sample were used for quantitative real-time PCR, which

was performed using SYBR Green/fluorescein dye on a Bio-Rad iCycler (http://www.bio-rad.com/) according to the manufacturer's instructions. Gene expression was quantified using the method described by Pfaffl (2001). Primer pairs are listed in Table 2-1.

Acknowledgements

We thank Dr Edgar Spalding (Department of Botany, University of Wisconsin) for advice in developing the software, and adapting the imaging platform, Dr Zuyu Zheng (Plant Biology Laboratory, Salk Institute) for information concerning phyA shade phenotypes, and Dr Christian Fankhauser (Center for Integrative Genetics, University of Lausanne) for the pif4 pif5 double mutant line. Drs Yvon Jaillais, Ullas Pedmale, Dmitri Nusinow and Colleen Doherty provided critical feedback on this manuscript. This work was supported by grants from the National Institutes of Health (R01GM52413 to J.C. and R01GM56006 to S.A.K) and the National Science Foundation (IOS-0649389 to J.C.). B.C. was supported by an National Science Foundation Integrative Graduate Education and Research Traineeship (0504645). J.C. is an investigator of the Howard Hughes Medical Institute. Chapter 2 is a reproduction in full of the material as it appears in The Plant Journal, 2011. Cole, Benjamin; Kay, Steve A.; Chory, Joanne. Blackwell Publishing Ltd., 2011. The dissertation author was the primary investigator and author of this paper.

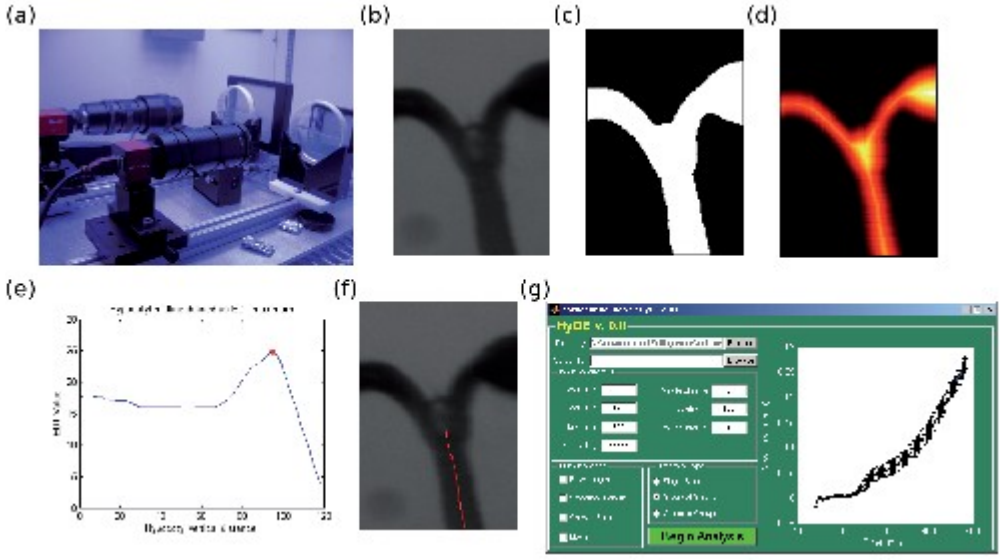

Figure 2-1: Image acquisition apparatus and image analysis software. (a) Two CCD cameras were set up to image plates, half-covered in growth media, under LED light conditions. (b) Whole images were cropped such that a single seedlings is visible, where the hypocotyl is the only structure present at the bottom. (c) The raw image is converted into binary format, and then the EDT is calculated (d). (e) A graph is constructed based on the value of the EDT at every hypocotyl midpoint along the vertical axis [rotated (d) 90° to the right], and a local maximum is selected indicating the centroid of the shoot apical meristem (red dot). (f) A line is drawn on the hypocotyl for every image in the stack for verification. (g) GUI for HYDE, illustrating the various features and parameters of the software.

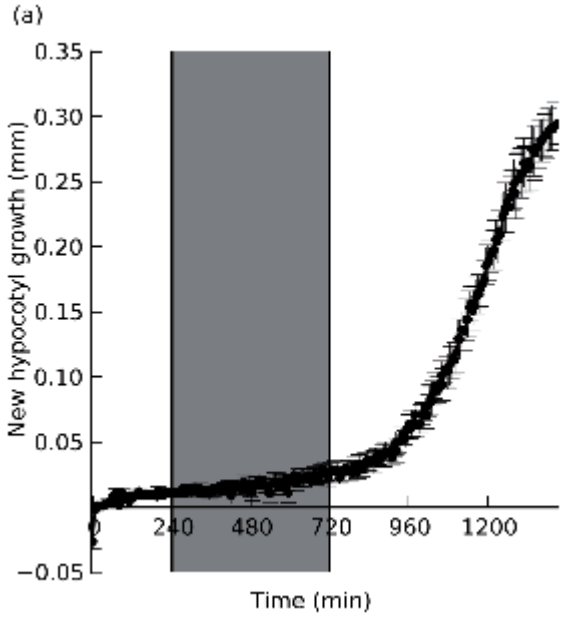

Figure 2-2: Circadian-regulated growth of WT seedlings released into LL. Col-0 seedlings entrained in 16 h/8 h light/dark cycles for 5 days were released into continuous control conditions starting at time 0 (ZT12). Subjective night is indicated in gray. Error bars indicate ±SEM for at least eight replicates.

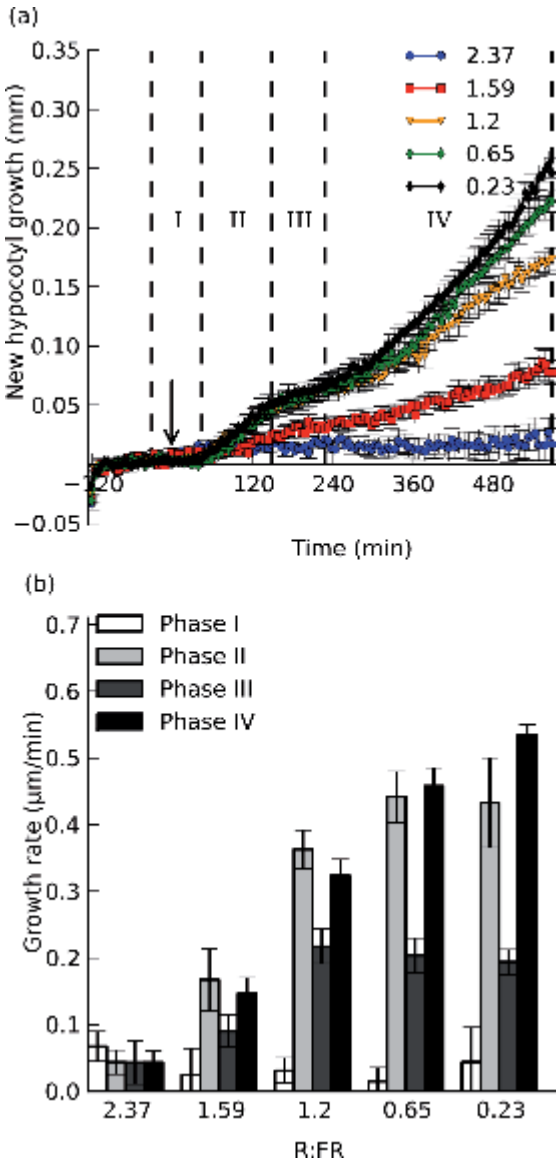

Figure 2-3: The magnitude of the growth response is inversely correlated with the R/FR ratio. Seedlings were exposed to varying intensities of supplemental FR light, and imaged for 2 h before exposure and 9.5 h after exposure. (a) New hypocotyl growth observed for seedlings exposed to supplemental FR light to give R/FR ratios of 0.23, 0.65, 1.2, 1.59 or 2.37 (control). The arrow indicates the start of treatment (t = 0). Dotted lines and Roman numerals indicate phases of growth for which growth rates are calculated in (b). (b) Growth rates calculated over selected time periods to reflect the various stages of growth. Error bars indicate the SEM for at least eight replicates in each assay.

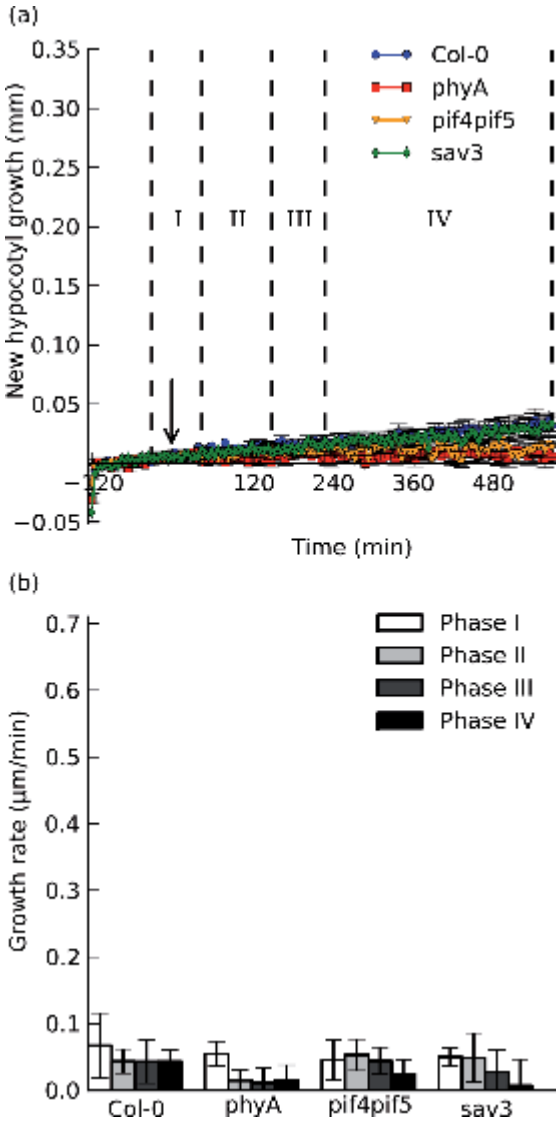

Figure 2-4: Growth of WT and mutant seedlings is negligible when kept in control conditions. Col-0, phyA-211, pif4-101pif5-1 and sav3-2 seedlings were maintained in the same pre-treatment conditions as before (see Figure 1), but not exposed to supplemental FR light. (a) New hypocotyl growth in WT, sav3, phyA, and pif4pif5 under control conditions (no supplemental FR). (b) Growth rates of (a) were calculated as in Figure 1.

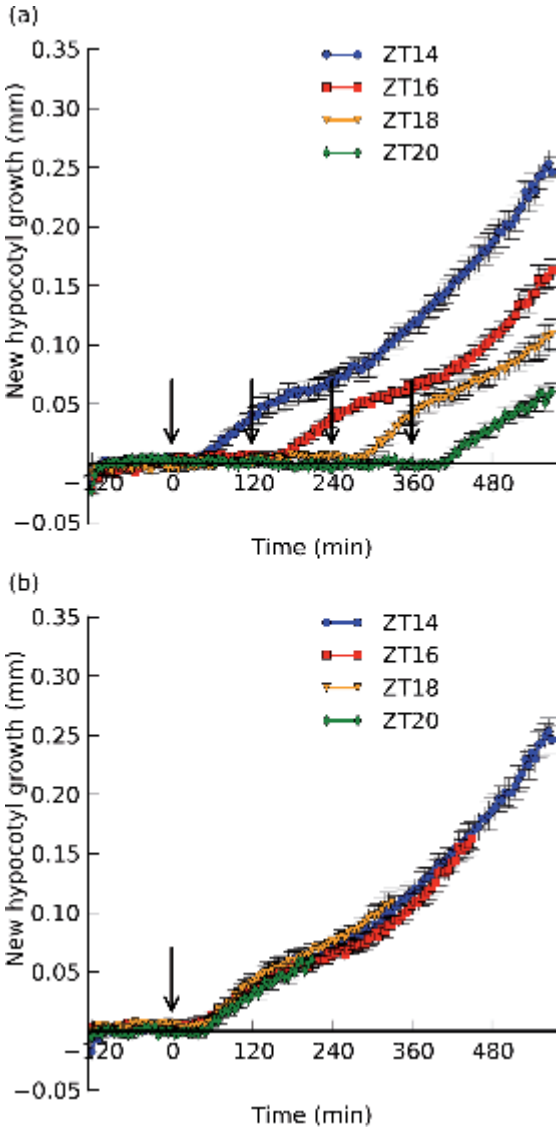

Figure 2-5: Altering the time of day at which shade treatment was applied has no effect on the shape or magnitude of the growth response. Col-0 seedlings were maintained under the same conditions as before (see Figure 1), but were kept under high R/FR for 2, 4 or 6 h longer than the original assay (treated with shade at ZT16, 18 or 20, respectively). Shown for reference is the ZT14 assay as described in Figure 1. (a) Growth responses normalized to the time of transfer to the imaging platform. Treatment times are indicated by arrows (at 0 min for ZT14, 120 min for ZT16, 240 min for ZT18, and 360 min for ZT20). (b) Curves normalized to the time of treatment (indicated by the arrow). Data were truncated prior to 120 min before treatment. Error bars indicate the SEM for at least six replicates.

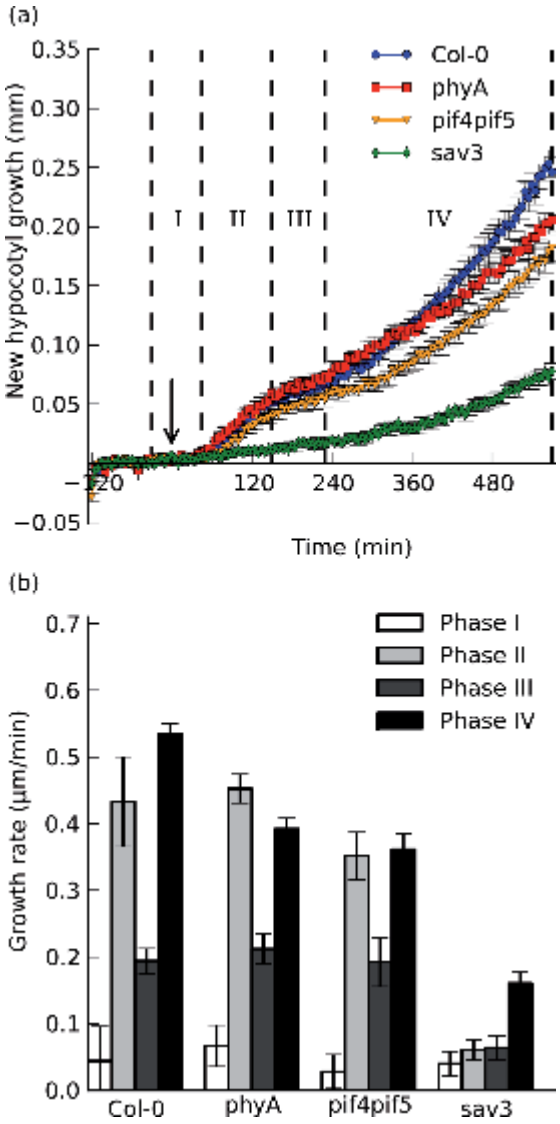

Figure 2-6: Shade-induced growth occurs in multiple distinct phases at the end of the day. (a) Shade-induced growth of wild-type (Col-0), *phyA-211* (phyA), *sav3-2* (sav3) and *pif4-101pif5-1* (pif4pif5). Supplemental FR treatment was performed after 2 h of acclimatization (indicated by the arrow) at t = 0. Seedlings were monitored for an additional 9.5 h after exposure to shade. Phases of growth are indicated by Roman numerals and dotted lines. (b) Growth rates were calculated for defined periods after shade exposure. Error bars represent the SEM for at least eight replicates in each assay.

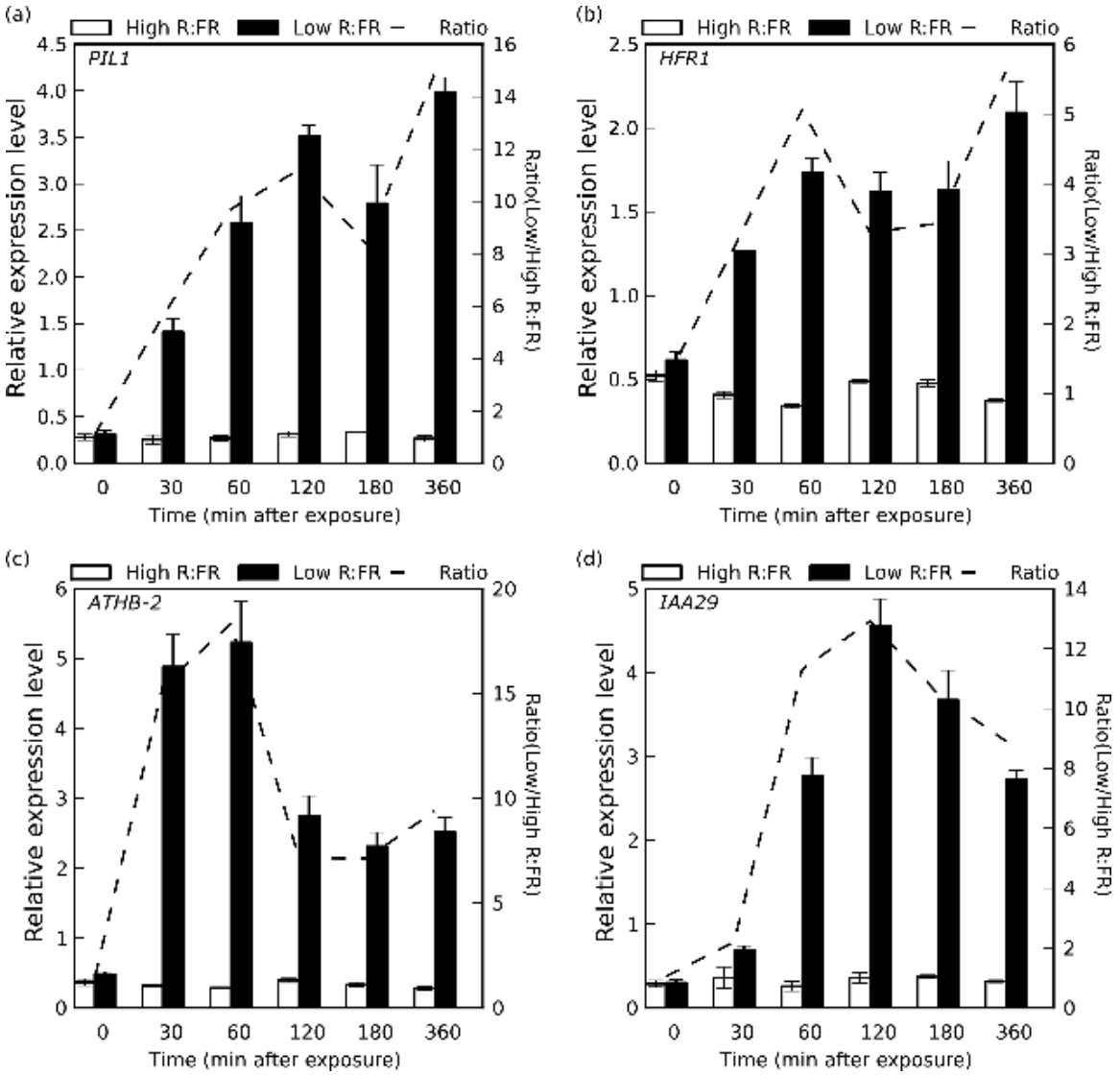

Figure 2-7: Gene expression patterns of shade marker genes correlate with hypocotyl growth phenotype. Col-0 seedlings were transferred into two separate chambers 2 h prior to treatment under identical light conditions. One chamber was treated with supplemental FR at time 0, reducing the R/FR to 0.23 (low R/FR), while the other remained under control conditions (high R/FR). Tissue was harvested for RNA extraction at each time point indicated. Quantitative real-time PCR was performed for (a) PIL1, (b) HFR1, (c) ATHB-2 and (d) IAA29. Error bars indicate the SEM for three biological replicates. The dotted line indicates the ratio (high/low R/FR) for each time point, and is plotted against a secondary y axis (indicated on the right).

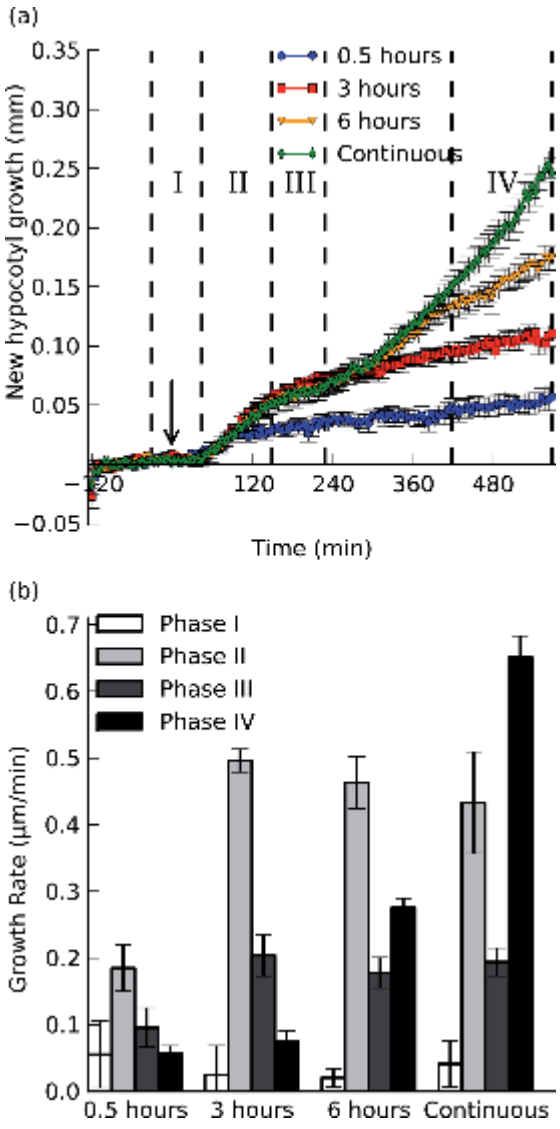

Figure 2-8: Elongation growth during shade is reversible by treatment under high R/FR light for at least 3 h. Seedlings were grown as described (see Materials and Methods), and treated with varying durations of low R/FR (0.23) light before reversion to the high R/FR (2.37) control level. (a) New hypocotyl growth (mm) plotted as a function of time for three treatments (continuous shade values from Figure 1 are included for comparison). The arrow indicates the start of shade treatment (t = 0). Dotted lines indicate phases of growth. The last phase has a different definition than in Figures 1 and 3 due to the close juxtaposition between the start of phase IV and the change of light treatment. (b) Growth rates measured over phases defined in (a): baseline rate (phase I, 30 min before treatment to 45 min after the start of treatment), the first elongation phase (phase II, 45–150 min after the start of treatment), the slowdown phase (phase III, 150–230 min after the start of treatment), and part of the second elongation phase (phase IV, 420–570 min after the start of treatment) chosen to highlight differences between the 6 h and continuous treatments. Error bars indicate the SEM for at least eight replicates in each assay.

Table 2-1: Primers for gene expression experiments. All quantitative real-time PCR experiments were performed using a melting temperature (Tm) of 60 °C and a 2-step protocol (60 s at 60 °C, 60 s at 95 °C for 39 cycles).

Gene Name	Forward / Reverse Primer Sequence
PIL1	TGGACTAATTCCAAACACTCCTATCTT / CACACGAAGGCACCACGA
ATHB-2	ACCATGTGCCCTTCATGTGA / CTGACGTAGCAGCCTGAGGTT
HFR1	GATGCCATCGCCGCTAATT / GTAAACGGTGGTAATGGCCAAT
IAA29	TCGAGGGTGCTGCGTCTT / TCGCCTCAAAACGCAGTTTT
IPP2	GTATGAGTTGCTTCTCCAGCAAAG / GAGGATGGCTGCAACAAGTGT

CHAPTER 3

Shade-induced hypocotyl dynamics in Arabidopsis depend on brassinosteroid signaling

Benjamin J. Cole, Yvon Jaillais, Steve A. Kay and Joanne Chory

Abstract

Competition for light is a constant struggle for plants, so much so, as they have evolved to be able to detect the threat of potentially shading vegetative neighbors (via a reduction in the R/FR ratio), and respond via apical growth and earlier transition into the reproductive stages of development. The Arabidopsis hypocotyl (which elongates with a characteristic multiphasic growth pattern in response to shade) has been adopted as a model for shade signal transduction. While phytohormone action has been implicated in shade regulated hypocotyl growth, the mechanisms which generate the multiple phases of elongation growth have not been fully characterized. Here, we report brassinosteroid (BR) signaling to play a role in promoting elongation growth in response to shade. We show that when BR biosynthesis is inhibited or when the BR receptor, BRI1 is impaired, hypocotyls fail to grow during the second major shade-induced elongation phase. We show that the BR signaling pathway is modulated in response to shade at the level of BES1 phosphorylation (the last step in the BR pathway), and expression of at least one BR-regulated gene is affected. As almost no elongation growth occurs when auxin transport is inhibited, we propose that BR signaling is activated as a consequence or in cooperation with auxin signaling, downstream of shade perception, to sustain growth during the latter stages of hypocotyl elongation. These results add new complexity to the already complex shade signaling pathway.

Introduction

For organisms wholly dependent on light for vitality, the threat of competition for this resource is not one to be taken lightly. As such, plants grown in high density respond through a characteristic suite of morphological changes (collectively known as the “shade avoidance syndrome”), most notably including elongation of hypocotyls, internodes, and petioles, restricted growth of storage organs (e.g. cotyledons and roots), and an earlier transition to the reproductive phase of development (Smith and Whitelam, 1997; Franklin, 2008). Plants use the ratio of red (R) to far-red (FR) light as an environmental light quality cue to discern whether they are being shaded, or whether shading vegetative growth is imminent, as the chlorophyll of potentially shading leaf tissue absorbs primarily in the red and blue photospectrum, and mostly transmits or reflects far-red light (Kasperbauer, 1987; Ballaré et al., 1990). This R/FR ratio shift is primarily perceived by the phytochrome class of photoreceptors, specifically *PHYTOCHROME B* (PHYB), PHYD, and PHYE (Franklin et al., 2003), as these photoreceptors can interconvert between red- and far-red light absorbing forms (Pr and Pfr, respectively) which differentially modulate phytochrome signal transduction (Smith, 2000). A great deal of genetic and biochemical studies have characterized this signaling pathway, which regulates processes ranging from germination, circadian clock entrainment, flowering, and shade avoidance (Franklin and Quail, 2010).

Much of the work done to date has focused on the *Arabidopsis thaliana* hypocotyl, due to its simple structure, ease of measurement, high light sensitivity, and reliance on cell elongation (rather than cell division) for much of its growth (Gendreau et al., 1997; Chen et al., 2004). The current model describes phytochrome B to be the principle red/far-red light photoreceptor that, when activated by red light, directly binds to and targets for degradation a subclass of bHLH transcription factors, known as

PHYTOCHROME INTERACTING FACTORS, or PIFs (Ni et al., 1998, 1999; Lorrain et al., 2008). Of these, PIF4 and PIF5 are thought to promote growth in response to shade (when the R/FR ratio drops, and phytochrome B is converted to its inactive Pr form), through modulation of gene expression and (together with PIF1 and PIF3) negatively regulate photomorphogenesis in the dark (Leivar et al., 2008; Shin et al., 2009). Gene expression studies have identified many genes strongly up-regulated by phytochrome signaling during shade avoidance, one of which, *LONG HYPOCOTYL IN FAR RED 1* (HFR1) negatively regulates shade avoidance responses, as *hfr1* mutant seedlings have longer hypocotyls in shade conditions (Fairchild et al., 2000; Sessa et al., 2005). HFR1 has been shown to comprise a negative feedback loop on the PIFs, as HFR1 protein can bind to PIF4 and PIF5, preventing its DNA binding capability (Hornitschek et al., 2009). Other negative regulators of shade similarly identified to be activated by the the low R/FR stimulus include *PHYTOCHROME INTERACTING FACTOR 3-LIKE 1* (PIL1), *PHYTOCHROME RAPIDLY REGULATED 1* (PAR1), and PAR2 (Salter et al., 2003; Roig-Villanova et al., 2006). A positive regulator, *ARABIDOPSIS THALIANA HOMEOBOX 2* (ATHB-2) has also been identified by these studies, which is auxin-inducible, and when mutated causes reduced hypocotyl elongation in response to low R/FR .

Auxin has recently been shown to play a central role in promoting elongation in response to shade, most directly via the *SHADE AVOIDANCE 3* mutation (*sav3)* which was identified in a genetic screen (Stepanova et al., 2008; Tao et al., 2008) for seedlings which fail to elongate their hypocotyls in response to low R/FR. *SAV3* (also known as *TRYPTOPHAN AMINOTRANSFERASE* 1 or *TAA1*) encodes an enzyme that catalyzes the conversion of tryptophan to indole-3-pyruvic acid (IPA), a critical step in auxin biosynthesis, and its lack of elongation during shade avoidance is echoed via treatment

with the polar auxin inhibitor, 1-naphthylphthalamic acid, or NPA (Stepanova et al., 2008; Tao et al., 2008; Mashiguchi et al., 2011; Won et al., 2011). Using an image-based time course assay for hypocotyl growth, we have previously demonstrated that this rapid new auxin biosynthesis is necessary for the initiation of a multi-phasic hypocotyl elongation growth pattern. This pattern consists of two major elongation phases (the first of which is highly auxin-dependent), punctuated by a period of slower elongation growth (Cole et al., 2011). How low R/FR causes this increase in auxin biosynthesis is not entirely understood, nor is it known the reason or mechanism for a slowing phase between two elongation phases upon exposure to shade. Hormone pathways other than that of auxin have been implicated in governing shade avoidance responses and may contribute to this dynamic growth pattern, including that of gibberllic acid (GA) via DELLA-mediated inhibition of PIF activity in the absence of GA (Pierik et al., 2004; de Lucas et al., 2008; Feng et al., 2008), ethylene (Pierik et al., 2004, 2009), and (in response to blue light depletion, another form of shade stimulis) brassinosteroids (Kozuka et al., 2010; Keller et al., 2011; Keuskamp et al., 2011). It is not known whether brassinosteroids play a role in mediating responses to low R/FR signals, or exactly how GA and BR act in concert with (or independently from) auxin signaling to regulate growth.

In this report, we describe a role for brassinosteroids in regulating shade-induced hypocotyl elongation within the context of a dynamic growth pattern, primarily acting during the second major elongation phase. We show that this effect is likely mediated by brassinosteroid biosynthesis, and manifests itself in a dynamic phosphorylation pattern of BES1, a key BR-regulated transcription factor (Yin et al., 2002; Vert and Chory, 2006). We also report mild transcriptional changes likely effected by BES1 are apparent during the slowing phase. These results add new complexity to the shade growth model, and offer a hypothesis as to why shade-induced elongation occurs with a dynamic pattern.

Results and Discussion

Negative Regulators, PIL1 and HFR1, do not strongly affect the low R/FR hypocotyl growth pattern

To understand what factor(s) may cause slowing in growth during the shade response, we examined two previously-characterized putative negative regulators of shade-induced growth, PIL1 and HFR1, both of which are rapidly up-regulated in response to shade (Salter et al., 2003; Sessa et al., 2005), thus making them good candidates for this phenotype Using an imaging-based time course assay for shade-induced hypocotyl elongation described previously (Cole et al., 2011), we analyzed hypocotyl growth dynamics of 5-day old light-grown *pil1* and *hfr1-4* mutant seedlings. Both *hfr1-4* and *pil1* mutant seedlings demonstrated a very slight increase in growth rate during the first growth phase (between 45 min. and 150 min.; Figure 3-1). However, neither mutant displayed any strong deviation from the multi-phasic growth pattern, showing similar lag times before the initial growth phase, severity of the slowing period, and timing or magnitude of the re-induction of growth. Overexpression of PIL1 caused a phenotype similar to that of the *pif4pif5* double mutant, more dramatically affecting the second elongation phase than the first, yet this overall growth pattern is qualitatively similar to wild-type (Figure 3-1). These data suggest that if HFR1 and PIL1 have a negative effect on the shade growth pathway, it is minor for the first several hours, or their functions are redundant. It has previously been suggested that HFR1 acts to repress shade-induced growth by binding to PIF5, inhibiting its DNA binding activity (and thus preventing any transcriptional activation or repression). It is possible that PIL1 acts in a similar fashion, however a direct interaction has not been shown. It is also possible

that the negative regulators, HFR1 and PIL1, act redundantly with other negative regulators, such as PAR1 and PAR2 to mediate the dynamic growth response. However, absent higher-order mutants in these components, we do not have sufficient evidence to support or discount this hypothesis. We also examined whether varying light conditions may also modulate the growth pattern observed. Instead of reducing the R/FR ratio by elevating the amount of FR, we achieved the same R/FR by lowering the abundance of R, and followed hypocotyl elongation growth as above. Upon reduction of R/FR in this way, we observed a marked increase in the growth rate of the first major elongation phase, however the timing, magnitude, or duration of both the slowing phase, as well as the second major elongation phase were unaffected (Figure 3-1). This phenotype comes in stark contrast to that incurred by lowering blue light irradiation, which we observed to not strongly increase hypocotyl elongation rates during the first 10 hours of treatment. Seedlings treated with both low R and low B light conditions responded similarly to those exposed to low R alone during the first major elongation phase, but also exhibited enhancement of the second major elongation phase as well. Low blue light has previously been shown to be sufficient for shade responses (Pierik et al., 2009; Keller et al., 2011; Keuskamp et al., 2011; Lian et al., 2011; Liu et al., 2011). These data suggest that different blue light signaling and low R/FR signaling operate with different kinetics, even though they manifest the same overall long-term phenotypes, and that a complex interaction exists between the two signaling pathways. Further, we predict that lowering R rather than raising FR to reduce the R/FR ratio may alter the kinetics of how auxin is mobilized, or how auxin-induced elongation growth is carried out, yet the difference in shade stimuli does not severely affect the overall growth pattern.

Brassinozole treatment strongly impairs second major elongation phase

We next turned to a pharmacological approach, using chemicals which inhibit the auxin, brassinosteroid, and gibberelic acid biosynthesis and/or transport pathways, to determine if the dynamic shade growth response is regulated by multiple hormones. We previously showed that, while auxin (via the TAA1 pathway) is necessary for hypocotyl growth initiation, some shade-induced growth does occur during the second major elongation phase in mutant seedlings (Cole et al., 2011). To determine if this response, too, was dependent on aspects of auxin signaling, we treated 5-day old light-grown seedlings with 1-naphthylphthalamic acid (NPA) which inhibits polar auxin transport (Morgan, 1964). prior to treatment with shade As shown in Figure 3-2, These seedlings exhibited almost no growth at all following shade treatment, suggesting that the residual growth observed previously in *sav3-2* mutant seedlings (Cole et al., 2011) is probably still auxin-dependent, yet may occur through mobilizing auxin which is present from other biochemical pathways (e.g. non-tryptophan dependent auxin biosynthesis). These data also suggest that auxin transport is absolutely required for rapid shade-induced growth. In a similar assay, we used a different drug, brassinazole (BRZ), a specific inhibitor of brassinosteroid biosynthesis (Asami et al., 2000). When treated with 5μM BRZ, wild-type seedlings still responded initially to the shade stimulus, growing at a rate approximately the same as seedlings treated with DMSO, and exhibiting the same slowing phase characteristic of the shade response (Figure 3-2). However, after slowing, BRZ-treated seedlings failed to re-initiate elongation, growing at about the same rate throughout the rest of the assay as they grew during the slowing phase. We saw a similar effect with wild-type seedlings treated with paclobutrazol (Figure 3-3), which inhibits gibberelic acid biosynthesis. However, as PAC inhibits cytochrome P450 monooxygenases, critical to both GA and BR biosynthesis, specific effects of PAC could

not be determined. These data suggest that brassinosteroid biosynthesis is also an important component of the shade avoidance response, however it is less important for growth initiation, and perhaps more important for more sustained growth afterwards. We cannot rule out that gibberellins may also act in this capacity, and elements of this pathway have indeed been shown to be involved in regulating PIF transcription factor activity (de Lucas et al., 2008; Feng et al., 2008) as well as elongation growth (Pierik et al., 2004).

Mutations in BRI1 affect growth pattern

To further investigate the specific role BRs play in shade avoidance, we imaged plants with mutated alleles of the leucine-rich repeat/receptor kinase protein, *BRASSINOSTEROID INSENSITIVE 1* (BRI1), the receptor which mediates brassinosteroid signaling (Li and Chory, 1997; Friedrichsen et al., 2000; He et al., 2000). One of these alleles (*bri1-301*) is a weak loss-of-function mutation in the BRI1 kinase domain, causing mild dwarfism in seedlings and adult plants (Xu et al., 0000). In image-based shade assays for hypocotyl elongation, bri1-301 seedlings showed a slight delay in slowing after the initial growth phase, however almost completely fail to elongate any further following this phase, unlike wild-type (Col-0) seedlings which elongate in the second major growth phase, as expected (Figure 3-4). Conversely, when we imaged a second mutant line expressing a dominant gain-of-function transgenic allele of BRI1 under the *UBIQUITIN 10* promoter (*UB10::BRI1*^{SUD1}*),* we saw a slight enhancement of growth during the second major elongation phase. This line also showed a slight delay in slowing during the first major elongation phase similar to that seen in *bri1-301* seedlings, yet we also observed that growth rates during the slowing phase (between 150 and 230 min after exposure) were elevated. Similar results were also observed

following treatment of a line overexpressing BKI1 (a negative regulator of BRI1 receptor kinase activity; (Wang and Chory, 2006) with shade (Figure 3-4). This line grew markedly less than wild-type seedlings during the both major elongation phases, yet still exhibited some growth during the initiation phase (unlike an the *sav3-2* mutant or seedlings treated with NPA). Taken together, these results strongly suggest that brassinosteroid biosynthesis and signaling are both required for a full elongation response to occur after shade exposure. Furthermore, we suspect that a transient attenuation of BR signaling may be one of the mechanisms mediating the slowing phase observed in shade-avoiding hypocotyls.

BES1 phosphorylation is dynamic in response to low R/FR

To determine whether the interaction between the brassinosteroid signaling pathway and shade responses is reflected at the molecular level, we assayed for BES1 phosphorylation over a 5-hour time course in 5-day old seedlings treated with shade. BIN2 (when active in the absence of brassinosteroids) keeps BES1 in a highly phosphorylated state, inactivating the transcription factor. This phosphorylation difference is apparent by a substantial electrophoretic mobility shift, easily detectable by blotting with an anti-BES1 antibody. In response to shade, we observed accumulation of unphosphorylated BES1 through the 2.5 hour timepoint. By 3 hours (while seedlings would slow their growth rates in our shade imaging assay), we observed a shift in phosphorylation state of BES1, where most of the protein was in its phosphorylated (and inactive) form, indicating a shut down of the brassinosteroid signaling pathway. This shift persists until 4.5 hours, when most of the protein returns to the dephosphorylated (active) state. These phosphorylation dynamics correlate with the observed growth patterns, indicating that the BR pathway is affected during shade avoidance. We also

assessed whether this shift in BES1 phosphorylation levels has any impact on transcription of BR-regulated genes. We chose DWF4 and CPD as a transcriptional readouts of BR pathway activation, as these gene are direct targets of BES1/BZR1, and are both down-regulated in response to brassinosteroid application. However, these genes make poor markers, as they both encode for brassinosteroid biosynthesis enzymes, and their down-regulation by BES1/BZR1 constitutes a negative feedback loop between signaling and hormone synthesis. Thus, any change at all in mRNA abundance from DWF4 and CPD can be construed as evidence either for, or against brassinosteroid pathway activation. Nonetheless, while CPD mRNA changes were not apparent (data not shown), we observed a very slight down-regulation of DWF4 during the timepoints at which hypocotyls are slowing in response to shade (2.5 hrs, 3hrs, and 3.5 hrs), however we also saw a slight down-regulation of DWF4 at the 2hr time point, which precedes both the hypocotyl slowing phase and the point at which BES1 becomes phosphorylated (Figure 3-4 and Figure 3-5). While based on this evidence we cannot conclude that loss of biosynthetic capacity is the cause of BES1 phosphorylation (and perhaps the slowing phase itself), this does pose an attractive hypothesis. It is equally possible that the BR signaling pathway is engaged in crosstalk with that of phytochrome, perhaps upstream of transcriptional modulation. Distinction between (or against both of) these models would necessitate more detailed study.

Conclusions

We have demonstrated here that low R/FR-induced hypocotyl elongation involves not just auxin and phytochrome signaling, but brassinosteroid signaling as well. We have shown that brassinazole treatment as well as mutations in the BRI1 brassinosteroid receptor have altered elongation growth phenotypes following exposure

to shade. We have also demonstrated that BR signaling is modulated by shade at the level of BES1 phosphorylation and downstream gene expression. Hormone pathways have long been known to play central roles in regulating shade responses, and while crosstalk between auxin and brassinosteroid signaling has been reported previously (Nemhauser et al., 2004; Vert et al., 2008), the temporal dynamics of how this interaction occurs has not yet been demonstrated. We believe that the first and second major elongation phases during the dynamic hypocotyl response to shade may represent respective contributions of auxin and brassinosteroid signaling, and that (at the physiological level) these two pathways are interdependent. Exactly what the regulatory point at which shade modulates brassinosteroid biosynthesis or signaling remains unclear, however we hope further work will serve to fill in these mechanistic details.

Materials and Methods

Plant growth and imaging

For imaging, protein, and RNA isolation experiements, Arabidopsis thaliana seeds were stratified for at least 2 days, then sown on ½ Murishige and Skoog (MS) media supplemented with 0.8% agar. For imaging assays, seeds were sown on top of ~730 µL of solid media in 1.1 mL cylindrical tubes (USA Scientific), molded with a 0.1-10 µL plastic pipette tip (USA Scientific) such that a short pedestal was formed on the agar surface. For all other assays, seedlings were sown on 24-well plates. Seedlings were grown under fluorescent white light (approx. 50 µE) in 16hr/8hr day/night photocycles for 5 days, and treated with shade (or control conditions) starting at ZT14 on the 5th day. Shade conditions are as described in Cole, et. al., (2011). Imaging and image analysis was performed as in Cole, et al. (2011) with some modifications: a custom-fitted round plexiglass sample holder (with a capacity of up to 48 samples/assay) was installed on a

50 mm rotation stage, which rotated the seedlings every 5 minutes, imaging each one individually. Image acquisition and motion were controlled using custom-designed software.

Drug treatments

1.5 hours prior to imaging, 5-day old light grown seedlings were flooded with either DMSO (in water), 5 μM NPA, 1 μM brassinazole, or various doses of paclobutrazol, and incubated for 1 hour. 30 minutes prior to imaging (or protein/RNA isolation), the liquid was removed, and the seedlings were loaded into the imaging chamber. Samples (or images) were taken at the indicated time points.

Protein and RNA isolation

Immediately after harvesting for protein or RNA isolation, seedlings were flash-frozen in liquid nitrogen, and processed or stored at -80C. RNA was isolated using a Plant RNA Isolation Kit (Sigma, St. Louis, MO, USA), and 1 μg was used as template for cDNA synthesis with a Maxima cDNA Synthesis kit (Fermentas, Burlington, ON, CA) according to the manufacturers' instructions. 5 μL of each 100x diluted cDNA sample was used for real-time quantitative PCR, performed using SYBR Green/Fluorescin on a CFX384 instrument (Bio-Rad; Hercules, CA USA) according to the manufacturer's instructions. Protein was isolated and boiled following tissue disruption with 4X sample buffer (50 mM Tris-Cl pH 6.8, 2% SDS, 10% glycerol, 1% 2-mercaptoethanol, 12.5 mM EDTA, and 0.02% bromphenol blue) for 5 minutes. Total protein extract was run on a 4-12% Bis-Tris gel (Life Technologies, San Diego, CA USA), and blotted onto nitrocellulose using standard procedures. BES1 was probed using anti-BES1 antibody (rabbit), followed by an IR780 dye conjugated to an anti-rabbit secondary antibody. Relative

protein abundance was imaged using the Odyssey Infrared Imager (Li-Cor, Lincoln, NE USA) according to the manufacturer's instructions.

Acknowledgements

We would like to acknowledge Dr. Yanhai Yin, who generously provided anti-BES1 antibody for these studies. We would also like to thank Dr. Gregory Vert and Dr. Ullas Pedmale for critical advice and suggestions. Funding was provided by an IGERT Plant Systems Biology fellowship to B.C., NIH(...) HHMI(...) to J.C. and Y.J., and NIH/NSF/DOE(...) to S.A.K. Chapter 3, in part, is being prepared for submission for publication of the material Cole, Benjamin J., Jaillais, Yvon, Kay, Steve A., Chory, Joanne. The dissertation author was the primary investigator and author of this material.

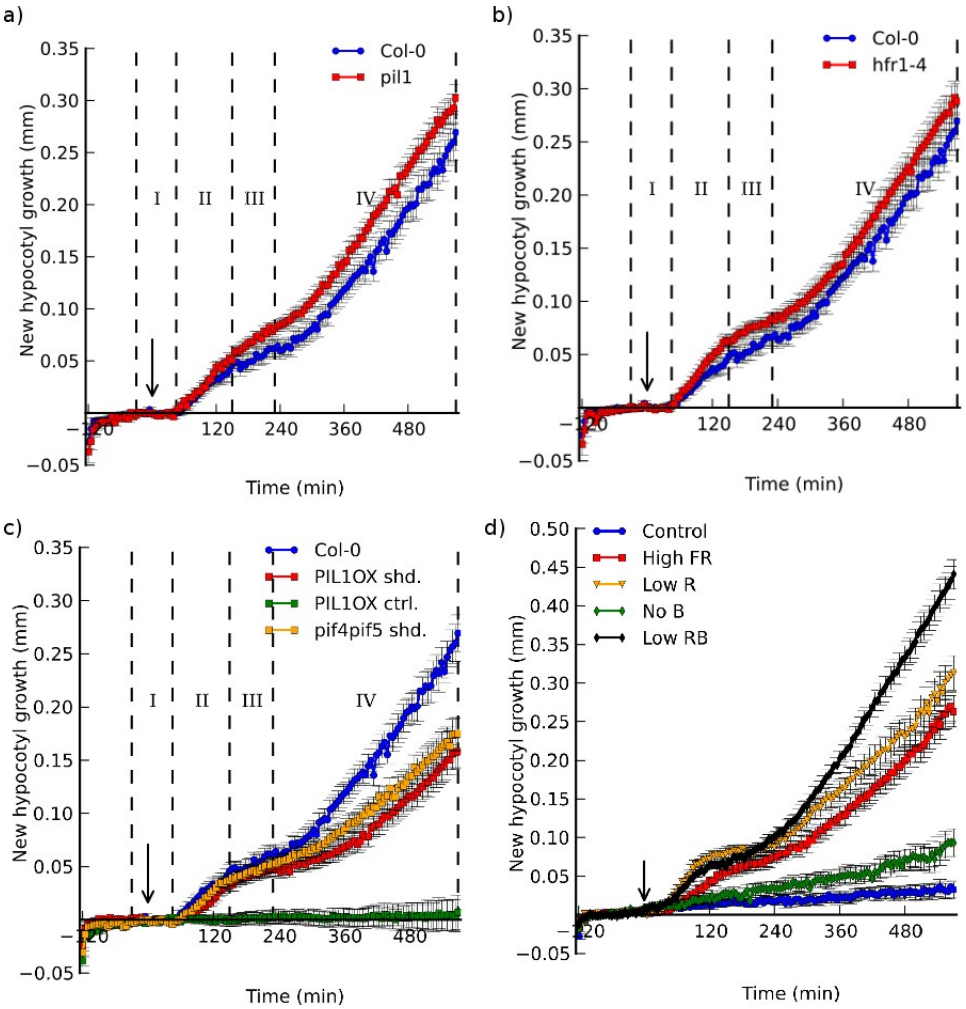

Figure 3-1: Hypocotyl growth kinetics are slightly influenced by negative regulators and different shade conditions. New hypocotyl length was measured from image stacks of pil1-101 (a T-DNA insertion null allele of PIL1; a) and hfr1-4 (a mutant allele of HFR which produces no transcript; b) seedlings, in response to shade conditions (supplemental FR such that the R/FR was 0.23), and compared to previously reported growth patterns of wild-type (Col-0) seedlings (Cole, et al., 2011). c) Hypocotyl growth kinetics of an overexpression allele of PIL1, PIL1-OX (red), in comparison with growth kinetics of wild-type (Col-0) and pif4-101pif5-1 double mutant seedlings (blue, and yellow, respectively; published previously; Cole, et al., 2011). Shown in green are PIL1-OX seedlings kept in high R/FR conditions. d) Hypocotyl growth patterns of wild-type seedlings exposed to supplemental FR (red), lowered R (yellow), lowered blue light (green), lowered red and blue light (black) or control (no change) conditions (blue). High FR, low R, and low red/low blue conditions all had R/FR ratio of ~0.23. Error bars represent ±s.e.m. for at least 8 biological replicates. Roman numerals in (a), (b), and (c) indicate various phases of growth as reported in Cole, et al., 2011. These phases are absent in (d) due to the dramatically different kinetics of the low B growth curve. Arrow indicates the time of treatment. Y-axis indicates new hypocotyl growth in mm.

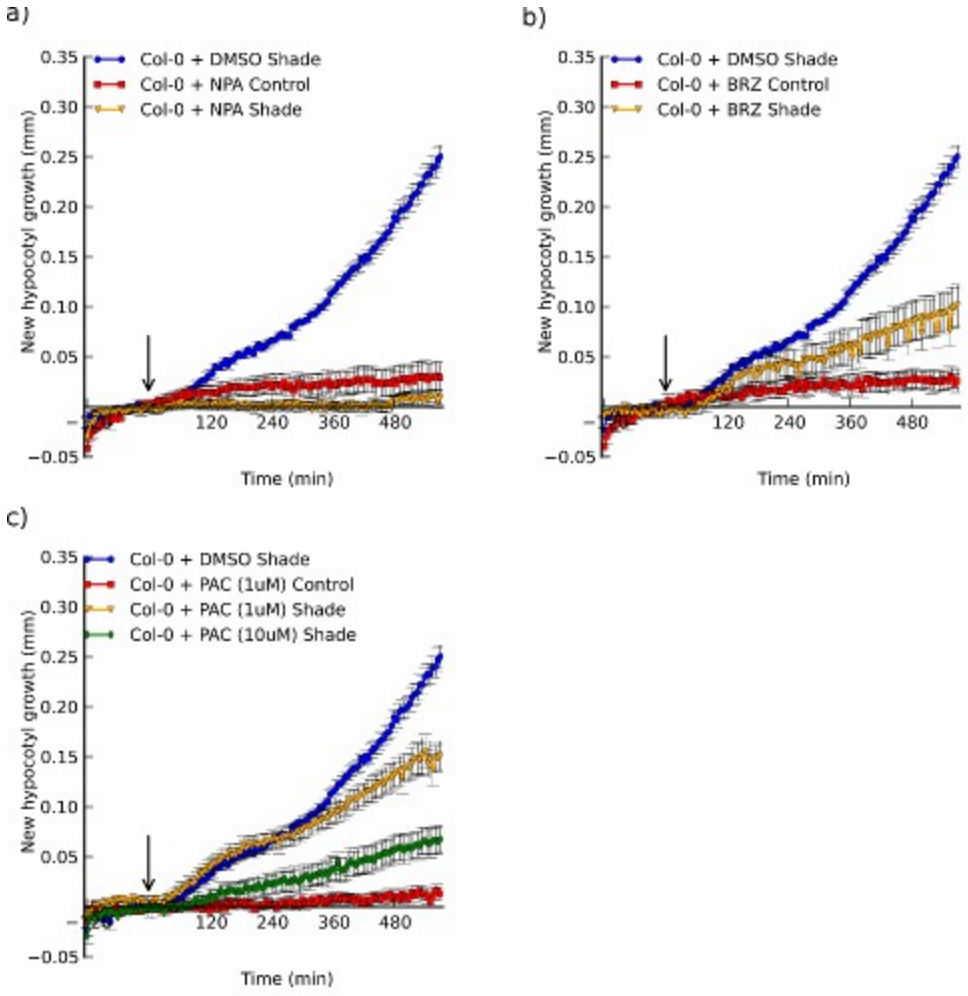

Figure 3-2: Hypocotyl growth kinetics in response to hormone pathway inhibitors. Wild-type (Col-0) seedlings were flooded with 5 μM NPA (a; yellow), 1 μM brassinazole (b; yellow), 0.1 (c; yellow) or 10 μM paclobutrazol (c; green) 1.5 hours prior to the start of imaging. Liquid was removed 0.5 hours prior to imaging. Seedlings were imaged and new hypocotyl length was measured as described previously (Cole, et al., 2011). Red lines indicate hypocotyl lengths of seedlings treated with the appropriate inhibitor in the absence of shade. Shade (supplemental FR, R/FR=0.23) was applied at time 0 (arrow). Error bars represent ±s.e.m. for at least 8 biological replicates. Y-axis indicates new hypocotyl growth in mm.

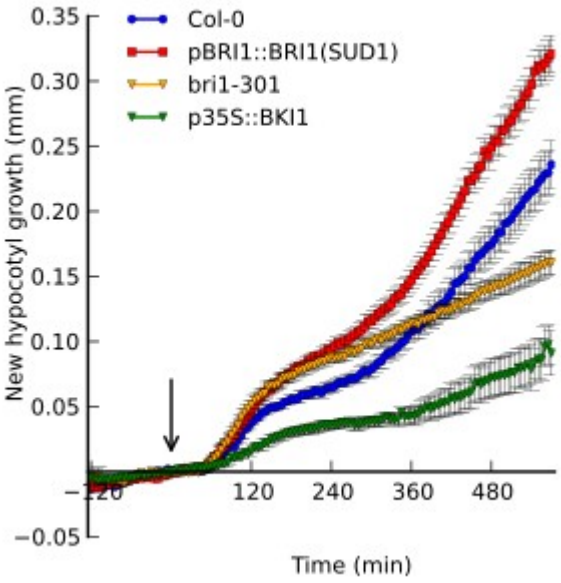

Figure 3-3: New hypocotyl growth of BRI1 alleles in response to shade. Wild-type (blue), *bri1-301* (yellow), pBRI1::BRI1^{SUD1} and 35S::BKI1-mCitrine (green) were imaged as described previously (Cole, et al., 2011). Arrow indicates the time of treatment, and the y-axis represents new hypocotyl growth in mm. Error bars represent ±s.e.m. for at least 8 biological replicates.

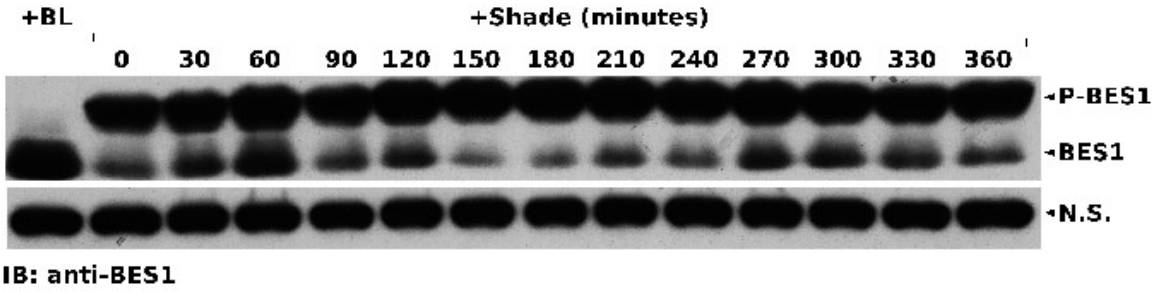

Figure 3-4: BES1 phosphorylation dynamics in response to shade. Wild-type seedlings (Col-0) were treated with shade (increased FR such that R/FR is 0.23) at time 0, and seedlings were harvested every 30 minutes for 6 hours. Protein extracts were probed with an anti-BES1 antibody, and phosphorylated (P-BES1) and de-phosphorylated (BES1) forms are distinguished by a differential electrophoretic mobility. This antibody cross-reacts with a non-specific band (N.S.) which is used here as a loading control. At the time of treatment, a separate collection of seedlings was treated with brassinolide (+BL), and these seedlings were harvested after 2 hours of shade treatment.

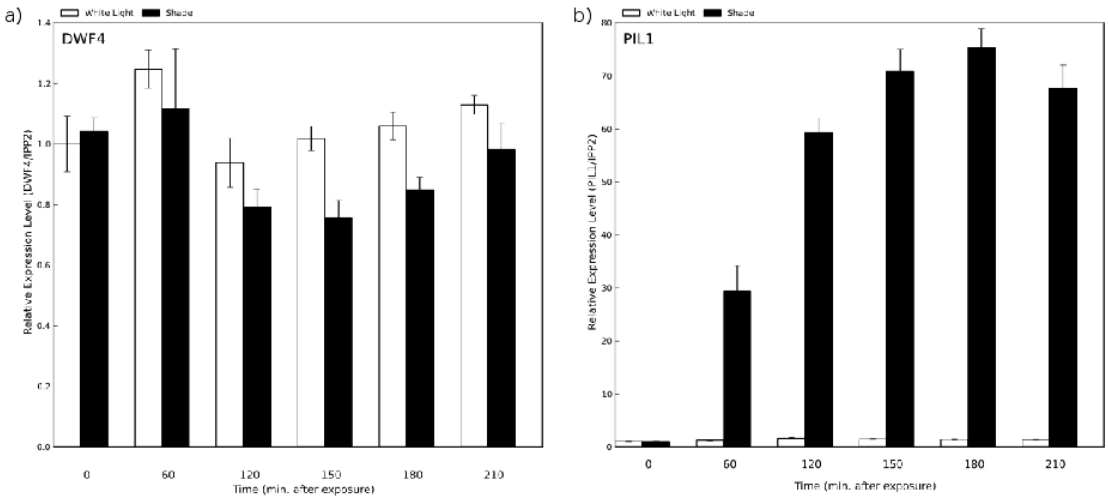

Figure 3-5 Gene expression profile of DWF4 and PIL1 in response to shade. RNA was extracted from 5-day old seedlings exposed to shade (black bars) or kept in control light conditions (white bars) for 0, 60, 120, 150, 180, and 210 minutes. Quantitative real-time PCR was performed as described (see Materials and Methods). Error bars indicate ±s.e.m. for 4 biological replicates (and 3 technical replicates).

PERSPECTIVES

This dissertation has focused on how dynamic phenotyping can serve to place multiple, seemingly-overlapping molecular process into a temporal framework. As plant research moves forward in uncovering ever-increasing degrees of complexity in signaling pathways, it will become important to consider how cellular process operate beyond static wiring diagrams and simplistic models. It is clear that spatio-temporal considerations must be taken into account when considering biological phenomenon, as organisms naturally exist in a 4-dimensional environment. This point is excellently exemplified by the circadian clock: measurement of a single phenotype under a given condition (which happens to be clock-regulated, along with ~30% of the transcriptome) can be completely different (opposite, even) depending on whether you decided to treat and sample in the morning vs. the evening. As signaling roles for various pathways become more nuanced, arbitrary time points (e.g. 1 hour after treatment) can thus no longer be employed, rather the temporal window to look for molecular mechanisms must be guided by physiological data (e.g. a visible phenotype), such that the molecular events can be more closely correlated with direct morphological changes. This is no less true when thinking about where events occur in space (cell or tissue types), which is the next technological frontier to be explored. Indeed, recent advances in tagging specific cell types combined with cell-sorting in the root have yielded tremendous advances in root cell development, especially when these approaches are combined with temporal resolution (Brady et al., 2007; Sozzani et al., 2010) These cell-type specific studies have now been extended to allow purification of whole nuclei without the cell-sorting step (Deal and Henikoff, 2011), offering the prospect of spatial resolution in non-root tissues. More simplistic methods to reduce cell-type complexity (e.g. free-hand

dissection of hypocotyls to determine tissue-specific responses to auxin) will also prove useful, as they can be more readily employed in many mutant backgrounds without the need for time-intensive construction of transgenic tools. However, Arabidopsis seedlings may prove to make poor models for these tissue-specific studies due to their small stature and delicate tissues. Other model systems (such as the dicot, *Brassica rapa* or the monocot and cereal model, *Brachypodium distachyon*) are likely much more amenable to tissue-specific studies as they are much larger, and thus physically easier to dissect.

Regardless the methods employed, several large questions loom in the future of the study of light regulation in plant development, stemming from the research presented here. First, what is the mechanistic role of the DET1 complex in regulating chromatin stability or transcriptional repression? While DET1 is associated with an E3 ligase complex, no substrate of this complex is known, nor is it known whether the E3 ligase activity of this complex is necessary for transcriptional repression. Given the increasing amount of evidence linking DET1 to chromatin modification, it is likely that the complex is regulating some chromatin modifying enzyme (e.g. an histone acetyltransferase or DNA methyltransferase), though its affect on chromatin may be more indirect.

Second, how does light modulate auxin levels (or that of any phytohormone, for that matter)? It has been suggested that the circadian clock can alter auxin levels through transcriptional reprogramming (Michael et al., 2008; Rawat et al., 2009). This transcriptional mechanism has also been suggested for the PIF transcription factors, linking auxin regulation to the clock and shade signaling (Nozue et al., 2011). Is this specific to shade and phytochrome B, or do similar modulations of phytohormones governed by the PIFs also occur during photomorphogenesis, and circadian growth? How quickly can a transcriptional cascade affect auxin levels, and where is this auxin

produced? Undoubtedly, researchers are currently working on addressing some of these points, and hopefully a map of PIF transcriptional activity on their target genes will soon emerge, however inaccuracy (and lack of spatial resolution) of *in vivo* auxin measurements is a critical shortcoming of current research which will need to be overcome to convincingly establish a mode of regulation.

Third, what is the mechanism by which the circadian clock gates the response to shade? The gating function of the clock was first suggested through cyclic transcriptional patterns of *PIL1*, mutation of which affected rhythmic hypocotyl growth patterns (Salter et al., 2003). An obvious point of integration between the clock and shade pathways is the PIF4 and PIF5 transcriptional regulators, as these are severely affected in clock outputs (Nozue et al., 2007), however the *pif4pif5* mutant double mutant shows a relatively mild phenotype in response to shade (Lorrain et al., 2008; Cole et al., 2011), suggesting other PIFs act redudantly (or independently from) PIF4 and PIF5 to control the shade transcriptional response. A separate model could be that clock- and shade-regulated hypocotyl elongation are really separate pathways (mediated by different sets of PIF transcription factors), and a gating phenotype is observed by the superposition of a rhythmic growth controlled by the clock, the strong growth promotion initiated by shade (via auxin production), and an upper limit as to how fast a hypocotyl can grow. These models could perhaps be distinguished by a more comprehensive set of dynamic phenotyping experiments which sampled shade-regulated growth at all times of the day (especially those times during which clock-regulated growth is most prominent).

Lastly, how does auxin or phytochrome signaling regulate brassinosteroid signaling? As discussed in this dissertation, the brassinosteroid pathway is attenuated during the slowing phase of shade-induced growth, and re-initiated during the second

major elongation phase, a dynamic pattern which could be targeted at the level of transcription (via modulation of BES1 targets), biosynthesis (through up- or down-regulation of BR biosynthetic genes), or signaling (via direct inhibition or activation of BR signaling components, such as BES1/BZR1, BIN2, or even the BRI1 receptor). As BES1/BZR1 are putative basic Helix-Loop-Helix transcription factors, the potential for dimerization with other bHLH proteins exists; it is especially tempting to speculate that BES1/BZR1 can interact directly with the PIFs in a similar fashion, modulating the activity of BES1/BZR1 target genes (among them, BR biosynthetic genes).

The light signaling field in plants is thus more exciting than ever, as the surge in technological innovation creates more hypotheses than it was designed to answer, and pathway kinetics become ever-more established. Now, efforts in describing the molecular mechanisms by which plants grow and produce must come to fruition in more dynamic computational models, which can be used to predict performance under a wide variety of growth conditions. It is hoped that information contained in these sophisticated models will be increasingly leveraged for biotechnological applications in the farms and fields of modern agriculture, making the support and sustained wealth of our population a reality.

APPENDIX A

Image-based analysis of light-grown seedling hypocotyls in Arabidopsis

Benjamin J. Cole and Joanne Chory

Abstract

Time-resolved hypocotyl length measurements in seedlings have the potential to greatly aid genetic studies looking at light, hormone, and circadian regulation of cell expansion. Recently, several computer-based tools have been developed to quantify hypocotyl length during photomorphogenesis and early seedling development. Here we detail a method for quantifying Arabidopsis seedling hypocotyls in an image-based assay, focusing on light-grown seedlings responding to shade conditions.

Introduction

Hypocotyls of seedlings serve multiple functions in development. Hypocotyl structure is very simple, consisting of files of up to 20 cells, which grow almost exclusively by cell expansion (as opposed to cell division) (Gendreau et al., 1997). When germinated under soil, hypocotyls expand to push the undeveloped photosynthetic organs up to the surface where they can intercept light and undergo photomorphogenesis (Chen et al., 2004). During photosynthetic growth, they connect the root system with the cotyledons and leaves of the plant, allowing nutrients, minerals, and signaling hormones to be transported to their sites of action, and their elongation is under circadian control (Nozue et al., 2007). Arabidopsis hypocotyls also elongate in

response to proximity stress, generated by the threat or onset of foliar shade, to re-position photosynthetic organs to a more optimal position (Franklin, 2008). This shade condition is most often associated with an altered quality of light, namely a decreased red to far-red light ratio (Kasperbauer, 1987; C L Ballaré et al., 1990). Thus, hypocotyl length serves as an incredibly useful readout for many aspects of light signaling, as this parameter tends to be inversely proportional to the amount of light available. The high responsiveness to the light environment and the simplistic nature of the hypocotyl has made it an obvious subject of many mutant screens aimed at identifying important molecular contributors to light signaling (Tao et al., 2008; Fairchild et al., 2000; Nagatani et al., 1993). It is thus useful to extend these studies of hypocotyl length to dynamic studies of growth rates and kinetics. To aid these studies, new assays have been developed (Cole et al., 2011; Miller et al., 2007; Wang et al., 2009) which can accurately quantify length and growth rate of hypocotyls in time-lapse images under various light conditions. Image-based assays are advantageous, being non-invasive, sensitive (with the help of high-resolution camera technology), and relatively easy to perform. Here, we describe a protocol for growing, imaging, and quantifying hypocotyl length in a time-resolved assay of Columbia seedlings encountering shade conditions.

Materials

It is important to keep all solutions sterile, as fungal or bacterial growth can affect growth dynamics and image quality.

Seedling Growth and Imaging Components

1. Solid Plant Growth Medium: 0.8% Agar, 1/2 Linsmaier and Skoog (LS) nutrients, 2.5 mM MES. Prepare by adding MES powder to 1/2 LS solution, pH to 5.7 with

5M KOH, and then add the agar powder. Autoclave solution for 20 minutes.

2. ~100 sterilized, stratified Col-0 seeds
3. Sterile pipettes for plating seeds
4. Circular petri dishes and semicircular sterile molds (fitting snugly into the petri dishes, such that half of the volume is occluded).
5. Long-term seedling growth chamber (Percival) with 2-4 cool white fluorescent bulbs and 2 incandescent light bulbs. Total fluence rate should be approximately 50 µmol•m-2•s-1, and the temperature is kept at 20°C.
6. Spectroradiometer
7. Dedicated imaging growth chamber (Percival) with a 3 channel LED light source (blue, red, far-red), whose light conditions are variable, but adjusted to match the long-germ seedling growth chamber conditions (calibrate with a spectroradiometer).
8. IR LED backlight source (>800 nm) (See Note 1)
9. High-resolution video camera (>1 megapixel) (See Note 2)
10. Sample Vessel and Mount (See Note 3)
11. Macro video zoom lens (See Note 4)

Image processing and analysis

1. Camera Control Software (See Note 5)
2. Hypocotyl Analysis Software (See Note 6)
3. ImageJ installed with the MultiStackReg plugin:

   (**http://www.stanford.edu/~bbusse/work/downloads.html**)

Methods

Seedling growth and imaging

1. Prepare solid growth medium on which to plate seeds (pouring molten agar solution into plate fitted with mold; see Note 3).
2. Plate seeds onto sample vessel, and cover each seed with a thin layer (small drop) of molten agar solution to ensure root submergence and support for apical growth.
3. Grow seedlings in diurnal growth conditions in long-term seedling growth chamber. For this assay, we use long-day (16 hrs light/8 hrs dark) growth conditions to keep hypocotyl length short initially (see Note 3) and keep the temperature at 20°C. Typically, hypocotyls are at their most dynamic developmental stage 4-7 days post-germination under these conditions.
4. On day 5 (or 1-2 days earlier or later, depending on the assay), transfer the seedlings to the dedicated imaging chamber, and mount the seedling vessels in front of the camera.
5. Begin video image capture. Parameters should be set using the control software such that an image of a single seedling is taken every 5-10 minutes. This can be accomplished by adjusting the frame rate and the number of frames between image capture events (see Note 5).
6. Image seedling growth for 2 hours under normal (simulated white-light) conditions to establish a base line.
7. After 2 hours, increase the intensity of the far-red light channel (this can be programmed into the LED chamber). Continue this treatment for up to 36 hours.

Image processing and analysis

1. Convert all images into 8-bit grayscale TIFF images using ImageJ (or a similar image processing program).
2. For each image stack (all time series images associated with a single seedling), align images using a non-seedling reference point (e.g. the agar surface adjacent to the seedling). ImageJ plugins are available for this task (see MultiStackReg).
3. Crop the aligned image such that only hypocotyl information is contained at the very bottom of the image. Some of the basal hypocotyl can be eliminated as dynamic length measurements need only new growth. Cotyledons can be cropped out, as this information is not important for determining hypocotyl length.
4. Measure hypocotyl length in the stack using image analysis software (see Note 6).
5. Manually inspect output from the software, taking care to eliminate growth curves, which do not accurately reflect the hypocotyl length seen in the image stack. This can be done by overlaying the mid-line information with the original set of images. Eliminate stacks where the line deviates from the hypocotyl termination point.
6. Report results in units of millimeters of new hypocotyl growth.

Notes

1. To enable imaging in darkness, it is necessary to have a light source that emits long wavelength infrared light (>800 nm), which plants are “blind” to, yet can still be detected on a CCD camera. The LED source we use emits at 880 nm, and we also installed a 790nm cutoff filter on the camera lens such that this is the only light source allowed into the CCD detector.

2. Here, we use a 1392x1050 pixel CCD camera, capable of imaging at least 1 frame/second. Any pre-existing filters on the camera itself that would prevent detection of long wavelengths were removed.
3. It is important that seedlings are oriented vertically (for normal growth experiments; special conditions may be necessary for gravitropism studies, e.g.). To accomplish this for light-grown seedlings, we use a circular petri dishhalf-filled with solid growth medium (facilitated by a semicircular plexiglass mold during pouring) and plate seeds on the ledge formed. In this way, the areal portion of the seedling is allowed to grow unobstructed in air while the roots are allowed to penetrate through the growth medium. We have found that if seedlings are grown on a full agar plate (no ledge created), frictional forces generated as the seedling grows upward tend to impede growth, or cause the hypocotyl and root system to move downward (complicating downstream image processing algorithms). Furthermore, we add a thin layer of “top-agar” to the seeds, ensuring that they have enough support for vertical growth as young seedlings. It also helps if the hypocotyls are relatively short (3-5mm) at the time of imaging, although this is not always possible (e.g. imaging a photoreceptor mutant or under short-day conditions). This sample vessel (the petri dish) must then be mounted vertically to prevent vibration and displacement. In our case, we had a custom sample mount fabricated. Alternatively, if higher-throughput imaging is desired, individual seedlings can be grown in cylindrical tubes (e.g. USA Scientific, 1.1 mL tubes). This eliminates problems associated with seedling orientation, as the tubes can be freely rotated. Special considerations are needed for preparation of the agar surface, and controlling condensation when growing seedlings in these tubes: we use 0.1-10 µL pipette tips (upside-down) to

mold the surface in the cylindrical tubes into a short pedestal (minimizing optical obstruction from the meniscus formed), and punch a small hole in the tube cap to allow gas exchange and to minimize humidity.

4. A lens capable of delivering in-focus images at >100 pixels/mm is helpful. The higher the zoom factor on the lens, the more pixels a seedling image will occupy, increasing the accuracy of downstream image processing algorithms.
5. Software is necessary for controlling the camera (notifying it when to take and save images). Often this software is provided by the camera's manufacturer, but in some cases, manual programming is necessary. If using a motion-control device in combination with video imaging (to increase throughput), custom-designed control software must be engineered such that image capture is coordinated with motion. Take care that the scale of the image is accurately determined (measure how many pixels per millimeter the image represents).
6. To reduce error associated with (sometimes subjective) measurements of hypocotyl length, computer-based software is needed. If you are designing your own tool for measurement, it is important to find some distinguishing feature of the start and end points of the structure to be measured. For measuring hypocotyl length in stacks described above, the start point is fixed (the cropped bottom of the hypocotyl image). The end point is the only parameter that must be determined for accurate measurement. HyDE is one software-based tool we developed to automate measurements, removing bias. This tool can be downloaded from http://cactus.salk.edu/hyde. This program uses information at the shoot-apical meristem to determine where the hypocotyl ends, and traces a mid-line from the hypocotyl base up to this point. Once identified, the program calculates the length of this mid-line, and reports these values for each image

successfully processed. For measuring hypocotyl length in etiolated seedlings, the reader is directed to HYPOTrace (12) (http://phytomorph.wisc.edu/software/hypotrace.php). These tools, as well as other software for phenotyping are also being made publicly available through the iPlant collaborative project (http://www.iplantcollaborative.org).

Acknowledgements

Appendix A, in part, has been submitted for publication of the material as it may appear as a book chapter in Methods in Molecular Biology, 2011; Cole, Benjamin J., Chory, Joanne. Humana Press 2011.

APPENDIX B

HyDE software user's guide

Benjamin J. Cole

Abstract

HyDE (Hypocotyl Determining Engine) is a simple matlab-based program that measures hypocotyl growth in time-series images. The program will output raw length, smoothened length, and growth rate numerical data (though this feature is not implemented yet), as well as avi movies showing where the algorithm has predicted the hypocotyl to be. You can download HyDE from the web (http://cactus.salk.edu/hyde), or use a pre-compiled version installed through the iPlant collaborative (http://www.iplantcollaborative.org).

Installation

To use HyDE, you must first install the MATLAB Component Runtime compiler, which should be included with the distribution. Simply double-click the MCRinstaller.exe (windows users) or the MCRinstaller.dmg (mac users) file to begin installation. Once installed, open the HyDEv1_0win32.exe file (windows) or the HyDEv1_0macOSX.sh file (you may need to run this file in the terminal) to launch the application. Test the software on the images provided to ensure it is working properly (the software may take a while to load).

Image Pre-Processing

Input to HyDE requires one or more image stacks that have been pre-cropped in

ImageJ or some similar software. Ideally, images should be cropped so that only hypocotyl tissue is visible at the very base (no interfering cotyledon or petiole tissue). Other structures can be tolerated in other areas of the image, but the very bottom row of pixels should contain only hypocotyl information. This is true for all images in the stack. The entire seedling need not be present in the picture, but the shoot apical meristem and hypocotyl must be visible in all images in each stack, as the software will use bulge information in the meristem to find the hypocotyl termination point. Please refer to the test images provided to gauge how your images should look.

Directory Type

HyDE can be operated in three different major modes ("Single Stack", "Group of Stacks", "Group of Groups"), reflecting the type of folder hierarchy that is input to the program. Which setting you use will depend on your data storage scheme, or the number/type of image stacks you wish to analyze at once.

"Single Stack"

In the most basic case, only the Stack folders are necessary, in which case "Single Stack" should be selected, and the input will be the name of the folder containing one image stack. Here, graphical output will be the raw length data for the single stack (no error bars included).

"Group of Stacks"

If a whole set of seedlings need to be processed, select "Group of Stacks", and the folder containing all seedling stack folders should be selected as the input, reflecting a complete set of, for example, 10 seedlings of one genotype across a single condition. Here, the graphical output will be a single line (raw length data) with error bars, reflecting

the standard error of the mean at each time point.

“Group of Groups”

If the entire experiment needs to be analyzed at once, select “Group of Groups” as the input, and the program will process a set of sets of seedling stacks. Graphical output will be multiple lines, reflecting each a different stack type, with error bars indicating the standard error of the mean at each time point.

Input Parameters

All assay parameters are required for the program to proceed. They are described as follows:

“Start Time” This is used in defining the x-axis for the graphic (left edge of x-axis is “Start Time – Treat Time”). Usually, setting this to 0 is suitable.

“Treat Time” This is the time (in minutes) after “Start Time” that the treatment occurs, for setting the x-y intercept point. For some experiments, this may not be applicable, in which case, simply enter 0 (or the start time).

“End Time” This is the total amount of time (in minutes) that the experiment lasts. For example, for a 4 hour experiment, enter “240”. The program will expect an appropriate number of frames, given the “Minutes/Frame” parameter.

“Minutes/Frame” Simply the number of minutes between each frame (regardless of what time step you wish to use).

“Pixels/mm” The number of pixels per millimeter in the image.

“Frames/interval” This indicates whether the program will process every, ever other, every third, etc. frame in the stack. Entering “1” will process every image, while “2” will process every other image.

“Assay Tag” This is a string that will appear in all output files from the run.

Output options

This is what the program will return once its finished analyzing the data. Check the boxes to indicate how much output is needed. If nothing is checked, the program will still return a graphic indicating the relevant curves.

“Raw Length” This is the unprocessed length that is found on every frame. Output is in csv format, with a header row indicating from which plate/seedling the curve originated from. Some values may be omitted, due to too much fluctuation.

“Smoothened Length” This is the spline-fitted length curve for each seedling, for subsequently determining growth rate.

“Growth Rate” This is the derivative of the length smoothing spline for each seedling.

“Movie” This is the single-seedling movie, a compendium of each frame in the stack, with a red line indicating where the software thinks the hypocotyl is.

REFERENCES

Ahmad, M., and Cashmore, A.R. (1993). HY4 gene of A. thaliana encodes a protein with characteristics of a blue-light photoreceptor. Nature *366*, 162–166.

Ang, L.H., and Deng, X.W. (1994). Regulatory Hierarchy of Photomorphogenic Loci: Allele-Specific and Light-Dependent Interaction between the HY5 and COP1 Loci. The Plant Cell Online *6*, 613–628.

von Arnim, A.G., and Deng, X.W. (1993). Ring finger motif of Arabidopsis thaliana COP1 defines a new class of zinc-binding domain. Journal of Biological Chemistry *268*, 19626–19631.

Asami, T., Min, Y.K., Nagata, N., Yamagishi, K., Takatsuto, S., Fujioka, S., Murofushi, N., Yamaguchi, I., and Yoshida, S. (2000). Characterization of Brassinazole, a Triazole-Type Brassinosteroid Biosynthesis Inhibitor. Plant Physiology *123*, 93–100.

Ballaré, C.L., Scopel, A.L., and Sánchez, R.A. (1990). Far-red radiation reflected from adjacent leaves: an early signal of competition in plant canopies. Science *247*, 329–332.

Bannister, A.J., and Kouzarides, T. (2011). Regulation of chromatin by histone modifications. Cell Res *21*, 381–395.

Benhamed, M., Bertrand, C., Servet, C., and Zhou, D.-X. (2006). Arabidopsis GCN5, HD1, and TAF1/HAF2 Interact to Regulate Histone Acetylation Required for Light-Responsive Gene Expression. The Plant Cell Online *18*, 2893–2903.

Benvenuto, G., Formiggini, F., Laflamme, P., Malakhov, M., and Bowler, C. (2002). The photomorphogenesis regulator DET1 binds the amino-terminal tail of histone H2B in a nucleosome context. Curr. Biol. *12*, 1529–1534.

Brady, S.M., Orlando, D.A., Lee, J.-Y., Wang, J.Y., Koch, J., Dinneny, J.R., Mace, D., Ohler, U., and Benfey, P.N. (2007). A high-resolution root spatiotemporal map reveals dominant expression patterns. Science *318*, 801–806.

Briggs, W.R., Beck, C.F., Cashmore, A.R., Christie, J.M., Hughes, J., Jarillo, J.A., Kagawa, T., Kanegae, H., Liscum, E., Nagatani, A., et al. (2001). The Phototropin Family of Photoreceptors. The Plant Cell Online *13*, 993–997.

Butler, W.L., Norris, K.H., Siegelman, H.W., and Hendricks, S.B. (1959). DETECTION, ASSAY, AND PRELIMINARY PURIFICATION OF THE PIGMENT CONTROLLING PHOTORESPONSIVE DEVELOPMENT OF PLANTS. Proc Natl Acad Sci U S A *45*, 1703–1708.

Carabelli, M., Morelli, G., Whitelam, G., and Ruberti, I. (1996). Twilight-zone and canopy shade induction of the Athb-2 homeobox gene in green plants. Proc. Natl. Acad.

Sci. U.S.A. *93*, 3530–3535.

Casal, J.J. (1996). Phytochrome A enhances the promotion of hypocotyl growth caused by reductions in levels of phytochrome B in its far-red-light-absorbing form in light-grown Arabidopsis thaliana. Plant Physiol. *112*, 965–973.

Casal, J.J., and Smith, H. (1988). Persistent effects of changes in phytochrome status on internode growth in light-grown mustard: Occurrence, kinetics and locus of perception. Planta *175*, 214–220.

Casal, J.J., and Smith, H. (1989). The “end-of-day” phytochrome control of internode elongation in mustard: kinetics, interaction with the previous fluence rate, and ecological implications. Plant, Cell & Environment *12*, 511–520.

Castells, E., Molinier, J., Benvenuto, G., Bourbousse, C., Zabulon, G., Zalc, A., Cazzaniga, S., Genschik, P., Barneche, F., and Bowler, C. (2011). The conserved factor DE-ETIOLATED 1 cooperates with CUL4-DDB1DDB2 to maintain genome integrity upon UV stress. EMBO J *30*, 1162–1172.

Chapman, E.J., and Estelle, M. (2009). Mechanism of Auxin-Regulated Gene Expression in Plants. Annual Review of Genetics *43*, 265–285.

Chen, H., Shen, Y., Tang, X., Yu, L., Wang, J., Guo, L., Zhang, Y., Zhang, H., Feng, S., Strickland, E., et al. (2006). Arabidopsis CULLIN4 Forms an E3 Ubiquitin Ligase with RBX1 and the CDD Complex in Mediating Light Control of Development. Plant Cell *18*, 1991–2004.

Chen, M., Chory, J., and Fankhauser, C. (2004). Light signal transduction in higher plants. Annu. Rev. Genet *38*, 87–117.

Chen, M., Tao, Y., Lim, J., Shaw, A., and Chory, J. (2005). Regulation of phytochrome B nuclear localization through light-dependent unmasking of nuclear-localization signals. Curr. Biol. *15*, 637–642.

Child, R., and Smith, H. (1987). Phytochrome action in light-grown mustard: kinetics, fluence-rate compensation and ecological significance. Planta *172*, 219–229.

Chory, J., Peto, C., Feinbaum, R., Pratt, L., and Ausubel, F. (1989). Arabidopsis thaliana mutant that develops as a light-grown plant in the absence of light. Cell *58*, 991–999.

Christie, J.M., Reymond, P., Powell, G.K., Bernasconi, P., Raibekas, A.A., Liscum, E., and Briggs, W.R. (1998). Arabidopsis NPH1: a flavoprotein with the properties of a photoreceptor for phototropism. Science *282*, 1698–1701.

Cole, B., Kay, S.A., and Chory, J. (2011). Automated analysis of hypocotyl growth dynamics during shade avoidance in Arabidopsis. Plant J *65*, 991–1000.

Cosgrove, D.J. (1982). Rapid inhibition of hypocotyl growth by blue light in Sinapis alba L. Plant Science Letters *25*, 305–312.

Deal, R.B., and Henikoff, S. (2011). The INTACT method for cell type-specific gene expression and chromatin profiling in Arabidopsis thaliana. Nat Protoc *6*, 56–68.

Deng, X.W., Caspar, T., and Quail, P.H. (1991). cop1: a regulatory locus involved in light-controlled development and gene expression in Arabidopsis. Genes Dev. *5*, 1172–1182.

Deng, X.W., Matsui, M., Wei, N., Wagner, D., Chu, A.M., Feldmann, K.A., and Quail, P.H. (1992). COP1, an Arabidopsis regulatory gene, encodes a protein with both a zinc-binding motif and a G beta homologous domain. Cell *71*, 791–801.

Devlin, P.F., Yanovsky, M.J., and Kay, S.A. (2003). A genomic analysis of the shade avoidance response in Arabidopsis. Plant Physiol. *133*, 1617–1629.

Djakovic-Petrovic, T., de Wit, M., Voesenek, L.A.C.J., and Pierik, R. (2007). DELLA protein function in growth responses to canopy signals. Plant J. *51*, 117–126.

Doherty, C.J., and Kay, S.A. (2010). Circadian Control of Global Gene Expression Patterns. Annual Review of Genetics *44*, 419–444.

Duek, P.D., and Fankhauser, C. (2003). HFR1, a putative bHLH transcription factor, mediates both phytochrome A and cryptochrome signalling. Plant J. *34*, 827–836.

Fairchild, C.D., Schumaker, M.A., and Quail, P.H. (2000). HFR1 encodes an atypical bHLH protein that acts in phytochrome A signal transduction. Genes & Development *14*, 2377–2391.

Feng, S., Martinez, C., Gusmaroli, G., Wang, Y., Zhou, J., Wang, F., Chen, L., Yu, L., Iglesias-Pedraz, J.M., Kircher, S., et al. (2008). Coordinated regulation of Arabidopsisthaliana development by light and gibberellins. Nature *451*, 475–479.

Folta, K.M., and Spalding, E.P. (2001). Opposing roles of phytochrome A and phytochrome B in early cryptochrome-mediated growth inhibition. The Plant Journal *28*, 333–340.

Franklin, K.A. (2008). Shade avoidance. New Phytol *179*, 930–944.

Franklin, K.A., and Quail, P.H. (2010). Phytochrome functions in Arabidopsis development. J. Exp. Bot. *61*, 11–24.

Franklin, K.A., Praekelt, U., Stoddart, W.M., Billingham, O.E., Halliday, K.J., and Whitelam, G.C. (2003). Phytochromes B, D, and E Act Redundantly to Control Multiple Physiological Responses in Arabidopsis. Plant Physiology *131*, 1340–1346.

Friedrichsen, D.M., Joazeiro, C.A., Li, J., Hunter, T., and Chory, J. (2000). Brassinosteroid-insensitive-1 is a ubiquitously expressed leucine-rich repeat receptor serine/threonine kinase. Plant Physiol. *123*, 1247–1256.

Fujimori, T., Yamashino, T., Kato, T., and Mizuno, T. (2004). Circadian-controlled basic/helix-loop-helix factor, PIL6, implicated in light-signal transduction in Arabidopsis thaliana. Plant Cell Physiol. *45*, 1078–1086.

García-Martínez, J.L., Keith, B., Bonner, B.A., Stafford, A.E., and Rappaport, L. (1987). Phytochrome Regulation of the Response to Exogenous Gibberellins by Epicotyls of Vigna sinensis. Plant Physiol. *85*, 212–216.

Gehring, M., Reik, W., and Henikoff, S. (2009). DNA demethylation by DNA repair. Trends in Genetics *25*, 82–90.

Gendreau, E., Traas, J., Desnos, T., Grandjean, O., Caboche, M., and Höfte, H. (1997). Cellular basis of hypocotyl growth in Arabidopsis thaliana. Plant Physiol *114*, 295–305.

Guo, L., Zhou, J., Elling, A.A., Charron, J.-B.F., and Deng, X.W. (2008). Histone Modifications and Expression of Light-Regulated Genes in Arabidopsis Are Cooperatively Influenced by Changing Light Conditions. Plant Physiology *147*, 2070–2083.

He, X.-J., Chen, T., and Zhu, J.-K. (2011). Regulation and function of DNA methylation in plants and animals. Cell Res *21*, 442–465.

He, Z., Wang, Z.Y., Li, J., Zhu, Q., Lamb, C., Ronald, P., and Chory, J. (2000). Perception of brassinosteroids by the extracellular domain of the receptor kinase BRI1. Science *288*, 2360–2363.

Hong, F., Breitling, R., McEntee, C.W., Wittner, B.S., Nemhauser, J.L., and Chory, J. (2006). RankProd: a bioconductor package for detecting differentially expressed genes in meta-analysis. Bioinformatics *22*, 2825–2827.

Hornitschek, P., Lorrain, S., Zoete, V., Michielin, O., and Fankhauser, C. (2009). Inhibition of the shade avoidance response by formation of non-DNA binding bHLH heterodimers. EMBO J. *28*, 3893–3902.

Hothorn, M., Belkhadir, Y., Dreux, M., Dabi, T., Noel, J.P., Wilson, I.A., and Chory, J. (2011). Structural basis of steroid hormone perception by the receptor kinase BRI1. Nature *474*, 467–471.

Huq, E., and Quail, P.H. (2002). PIF4, a phytochrome-interacting bHLH factor, functions as a negative regulator of phytochrome B signaling in Arabidopsis. EMBO J. *21*, 2441–2450.

Izaguirre, M.M., Mazza, C.A., Biondini, M., Baldwin, I.T., and Ballaré, C.L. (2006).

Remote sensing of future competitors: impacts on plant defenses. Proc. Natl. Acad. Sci. U.S.A. *103*, 7170–7174.

Jaillais, Y., and Chory, J. (2010). Unraveling the paradoxes of plant hormone signaling integration. Nat. Struct. Mol. Biol. *17*, 642–645.

Jaillais, Y., Hothorn, M., Belkhadir, Y., Dabi, T., Nimchuk, Z.L., Meyerowitz, E.M., and Chory, J. (2011). Tyrosine phosphorylation controls brassinosteroid receptor activation by triggering membrane release of its kinase inhibitor. Genes Dev. *25*, 232–237.

Ji, H., and Wong, W.H. (2005). TileMap: create chromosomal map of tiling array hybridizations. Bioinformatics *21*, 3629–3636.

Johnson, E., Bradley, M., Harberd, N.P., and Whitelam, G.C. (1994). Photoresponses of Light-Grown phyA Mutants of Arabidopsis (Phytochrome A Is Required for the Perception of Daylength Extensions). Plant Physiol. *105*, 141–149.

Kasperbauer, M.J. (1987). Far-Red Light Reflection from Green Leaves and Effects on Phytochrome-Mediated Assimilate Partitioning under Field Conditions. Plant Physiol *85*, 350–354.

Keller, M.M., Jaillais, Y., Pedmale, U.V., Moreno, J.E., Chory, J., and Ballaré, C.L. (2011). Cryptochrome 1 and phytochrome B control shade-avoidance responses in Arabidopsis via partially independent hormonal cascades. Plant J. *67*, 195–207.

Keuskamp, D.H., Sasidharan, R., Vos, I., Peeters, A.J.M., Voesenek, L.A.C.J., and Pierik, R. (2011). Blue-light-mediated shade avoidance requires combined auxin and brassinosteroid action in Arabidopsis seedlings. Plant J. *67*, 208–217.

Khanna, R., Huq, E., Kikis, E.A., Al-Sady, B., Lanzatella, C., and Quail, P.H. (2004). A novel molecular recognition motif necessary for targeting photoactivated phytochrome signaling to specific basic helix-loop-helix transcription factors. Plant Cell *16*, 3033–3044.

Kim, T.-W., Guan, S., Sun, Y., Deng, Z., Tang, W., Shang, J.-X., Sun, Y., Burlingame, A.L., and Wang, Z.-Y. (2009). Brassinosteroid signal transduction from cell-surface receptor kinases to nuclear transcription factors. Nat Cell Biol *11*, 1254–1260.

Kozuka, T., Kobayashi, J., Horiguchi, G., Demura, T., Sakakibara, H., Tsukaya, H., and Nagatani, A. (2010). Involvement of auxin and brassinosteroid in the regulation of petiole elongation under the shade. Plant Physiol. *153*, 1608–1618.

Kwok, S.F., Piekos, B., Misera, S., and Deng, X.W. (1996). A complement of ten essential and pleiotropic arabidopsis COP/DET/FUS genes is necessary for repression of photomorphogenesis in darkness. Plant Physiol. *110*, 731–742.

Lagarias, J.C., and Rapoport, H. (1980). Chromopeptides from phytochrome. The structure and linkage of the PR form of the phytochrome chromophore. J. Am. Chem. Soc. *102*, 4821–4828.

Lau, O.S., Huang, X., Charron, J.-B., Lee, J.-H., Li, G., and Deng, X.W. (2011). Interaction of Arabidopsis DET1 with CCA1 and LHY in Mediating Transcriptional Repression in the Plant Circadian Clock. Molecular Cell *43*, 703–712.

Leivar, P., Monte, E., Oka, Y., Liu, T., Carle, C., Castillon, A., Huq, E., and Quail, P.H. (2008). Multiple Phytochrome-Interacting bHLH Transcription Factors Repress Premature Seedling Photomorphogenesis in Darkness. Current Biology *18*, 1815–1823.

Lian, H.-L., He, S.-B., Zhang, Y.-C., Zhu, D.-M., Zhang, J.-Y., Jia, K.-P., Sun, S.-X., Li, L., and Yang, H.-Q. (2011). Blue-light-dependent interaction of cryptochrome 1 with SPA1 defines a dynamic signaling mechanism. Genes Dev. *25*, 1023–1028.

Li, B., Carey, M., and Workman, J.L. (2007). The Role of Chromatin during Transcription. Cell *128*, 707–719.

Li, J., and Chory, J. (1997). A putative leucine-rich repeat receptor kinase involved in brassinosteroid signal transduction. Cell *90*, 929–938.

Li, J., Nam, K.H., Vafeados, D., and Chory, J. (2001). BIN2, a New Brassinosteroid-Insensitive Locus in Arabidopsis. Plant Physiology *127*, 14–22.

Liscum, E., and Briggs, W.R. (1995). Mutations in the NPH1 locus of Arabidopsis disrupt the perception of phototropic stimuli. Plant Cell *7*, 473–485.

Lister, R., O'Malley, R.C., Tonti-Filippini, J., Gregory, B.D., Berry, C.C., Millar, A.H., and Ecker, J.R. (2008). Highly Integrated Single-Base Resolution Maps of the Epigenome in Arabidopsis. Cell *133*, 523–536.

Liu, B., Zuo, Z., Liu, H., Liu, X., and Lin, C. (2011). Arabidopsis cryptochrome 1 interacts with SPA1 to suppress COP1 activity in response to blue light. Genes Dev. *25*, 1029–1034.

Lorrain, S., Allen, T., Duek, P.D., Whitelam, G.C., and Fankhauser, C. (2008). Phytochrome-mediated inhibition of shade avoidance involves degradation of growth-promoting bHLH transcription factors. Plant J. *53*, 312–323.

de Lucas, M., Daviere, J.-M., Rodriguez-Falcon, M., Pontin, M., Iglesias-Pedraz, J.M., Lorrain, S., Fankhauser, C., Blazquez, M.A., Titarenko, E., and Prat, S. (2008). A molecular framework for light and gibberellin control of cell elongation. Nature *451*, 480–484.

Mashiguchi, K., Tanaka, K., Sakai, T., Sugawara, S., Kawaide, H., Natsume, M., Hanada, A., Yaeno, T., Shirasu, K., Yao, H., et al. (2011). The main auxin biosynthesis

pathway in Arabidopsis. Proceedings of the National Academy of Sciences of the United States of America.

Michael, T.P., Breton, G., Hazen, S.P., Priest, H., Mockler, T.C., Kay, S.A., and Chory, J. (2008). A Morning-Specific Phytohormone Gene Expression Program underlying Rhythmic Plant Growth. PLoS Biol *6*, e225.

Miller, N.D., Parks, B.M., and Spalding, E.P. (2007). Computer-vision analysis of seedling responses to light and gravity. Plant J *52*, 374–381.

Moreno, J.E., Tao, Y., Chory, J., and Ballaré, C.L. (2009). Ecological modulation of plant defense via phytochrome control of jasmonate sensitivity. Proc. Natl. Acad. Sci. U.S.A. *106*, 4935–4940.

Morgan, D.C., O'Brien, T., and Smith, H. (1980). Rapid photomodulation of stem extension in light-grownSinapis alba L. Planta *150*, 95–101.

Morgan, D.G. (1964). INFLUENCE OF ALPHA-NAPHTHYLPHTHALAMIC ACID ON THE MOVEMENT OF INDOLYL-3-ACETIC ACID IN PLANTS. Nature *201*, 476–477.

Nagashima, A., Suzuki, G., Uehara, Y., Saji, K., Furukawa, T., Koshiba, T., Sekimoto, M., Fujioka, S., Kuroha, T., Kojima, M., et al. (2008). Phytochromes and cryptochromes regulate the differential growth of Arabidopsis hypocotyls in both a PGP19-dependent and a PGP19-independent manner. Plant J. *53*, 516–529.

Nagatani, A., Reed, J.W., and Chory, J. (1993). Isolation and Initial Characterization of Arabidopsis Mutants That Are Deficient in Phytochrome A. Plant Physiol *102*, 269–277.

Nam, K.H., and Li, J. (2002). BRI1/BAK1, a receptor kinase pair mediating brassinosteroid signaling. Cell *110*, 203–212.

Nemhauser, J.L., Mockler, T.C., and Chory, J. (2004). Interdependency of Brassinosteroid and Auxin Signaling in Arabidopsis. PLoS Biol *2*, e258.

Ni, M., Tepperman, J.M., and Quail, P.H. (1998). PIF3, a phytochrome-interacting factor necessary for normal photoinduced signal transduction, is a novel basic helix-loop-helix protein. Cell *95*, 657–667.

Ni, M., Tepperman, J.M., and Quail, P.H. (1999). Binding of phytochrome B to its nuclear signalling partner PIF3 is reversibly induced by light. Nature *400*, 781–784.

Nozue, K., Covington, M.F., Duek, P.D., Lorrain, S., Fankhauser, C., Harmer, S.L., and Maloof, J.N. (2007). Rhythmic growth explained by coincidence between internal and external cues. Nature *448*, 358–361.

Nozue, K., Harmer, S.L., and Maloof, J.N. (2011). Genomic Analysis of Circadian Clock-,

Light-, and Growth-Correlated Genes Reveals PHYTOCHROME-INTERACTING FACTOR5 as a Modulator of Auxin Signaling in Arabidopsis. Plant Physiology *156*, 357–372.

Nusinow, D.A., Helfer, A., Hamilton, E.E., King, J.J., Imaizumi, T., Schultz, T.F., Farré, E.M., and Kay, S.A. (2011). The ELF4-ELF3-LUX complex links the circadian clock to diurnal control of hypocotyl growth. Nature *475*, 398–402.

Osterlund, M.T., Hardtke, C.S., Wei, N., and Deng, X.W. (2000). Targeted destabilization of HY5 during light-regulated development of Arabidopsis. Nature *405*, 462–466.

Parks, B.M., and Spalding, E.P. (1999). Sequential and coordinated action of phytochromes A and B during Arabidopsis stem growth revealed by kinetic analysis. Proceedings of the National Academy of Sciences *96*, 14142–14146.

Parks, B.M., Cho, M.H., and Spalding, E.P. (1998). Two Genetically Separable Phases of Growth Inhibition Induced by Blue Light in Arabidopsis Seedlings. Plant Physiology *118*, 609–615.

Pepper, A., Delaney, T., Washburn, T., Poole, D., and Chory, J. (1994). DET1, a negative regulator of light-mediated development and gene expression in arabidopsis, encodes a novel nuclear-localized protein. Cell *78*, 109–116.

Pierik, R., Cuppens, M.L.C., Voesenek, L.A.C.J., and Visser, E.J.W. (2004). Interactions between Ethylene and Gibberellins in Phytochrome-Mediated Shade Avoidance Responses in Tobacco. Plant Physiology *136*, 2928–2936.

Pierik, R., Djakovic-Petrovic, T., Keuskamp, D.H., de Wit, M., and Voesenek, L.A.C.J. (2009). Auxin and Ethylene Regulate Elongation Responses to Neighbor Proximity Signals Independent of Gibberellin and DELLA Proteins in Arabidopsis. Plant Physiology *149*, 1701–1712.

Premanandh, J. (2011). Factors affecting food security and contribution of modern technologies in food sustainability. Journal of the Science of Food and Agriculture *91*, 2707–2714.

Probst, A.V., Fagard, M., Proux, F., Mourrain, P., Boutet, S., Earley, K., Lawrence, R.J., Pikaard, C.S., Murfett, J., Furner, I., et al. (2004). Arabidopsis Histone Deacetylase HDA6 Is Required for Maintenance of Transcriptional Gene Silencing and Determines Nuclear Organization of rDNA Repeats. The Plant Cell Online *16*, 1021–1034.

Rawat, R., Schwartz, J., Jones, M.A., Sairanen, I., Cheng, Y., Andersson, C.R., Zhao, Y., Ljung, K., and Harmer, S.L. (2009). REVEILLE1, a Myb-like transcription factor, integrates the circadian clock and auxin pathways. Proc. Natl. Acad. Sci. U.S.A. *106*, 16883–16888.

Reed, J.W., Nagpal, P., Poole, D.S., Furuya, M., and Chory, J. (1993). Mutations in the

gene for the red/far-red light receptor phytochrome B alter cell elongation and physiological responses throughout Arabidopsis development. Plant Cell *5*, 147–157.

Rockwell, N.C., Su, Y.-S., and Lagarias, J.C. (2006). PHYTOCHROME STRUCTURE AND SIGNALING MECHANISMS. Annual Review of Plant Biology *57*, 837–858.

Roig-Villanova, I., Bou, J., Sorin, C., Devlin, P.F., and Martínez-García, J.F. (2006). Identification of primary target genes of phytochrome signaling. Early transcriptional control during shade avoidance responses in Arabidopsis. Plant Physiol. *141*, 85–96.

Rüdiger, W., Thümmler, F., Cmiel, E., and Schneider, S. (1983). Chromophore structure of the physiologically active form (P(fr)) of phytochrome. Proc. Natl. Acad. Sci. U.S.A. *80*, 6244–6248.

Sakamoto, K., and Nagatani, A. (1996). Nuclear localization activity of phytochrome B. Plant J. *10*, 859–868.

Salter, M.G., Franklin, K.A., and Whitelam, G.C. (2003). Gating of the rapid shade-avoidance response by the circadian clock in plants. Nature *426*, 680–683.

Schena, M., Lloyd, A.M., and Davis, R.W. (1993). The HAT4 gene of Arabidopsis encodes a developmental regulator. Genes Dev. *7*, 367–379.

Schroeder, D.F., Gahrtz, M., Maxwell, B.B., Cook, R.K., Kan, J.M., Alonso, J.M., Ecker, J.R., and Chory, J. (2002). De-Etiolated 1 and Damaged DNA Binding Protein 1 Interact to Regulate Arabidopsis Photomorphogenesis. Current Biology *12*, 1462–1472.

Schwechheimer, C., and Willige, B.C. (2009). Shedding light on gibberellic acid signalling. Curr. Opin. Plant Biol. *12*, 57–62.

Seo, H.S., Watanabe, E., Tokutomi, S., Nagatani, A., and Chua, N.-H. (2004). Photoreceptor ubiquitination by COP1 E3 ligase desensitizes phytochrome A signaling. Genes & Development *18*, 617–622.

Sessa, G., Carabelli, M., Sassi, M., Ciolfi, A., Possenti, M., Mittempergher, F., Becker, J., Morelli, G., and Ruberti, I. (2005). A dynamic balance between gene activation and repression regulates the shade avoidance response in Arabidopsis. Genes Dev. *19*, 2811–2815.

Shin, J., Kim, K., Kang, H., Zulfugarov, I.S., Bae, G., Lee, C.-H., Lee, D., and Choi, G. (2009). Phytochromes promote seedling light responses by inhibiting four negatively-acting phytochrome-interacting factors. Proceedings of the National Academy of Sciences *106*, 7660–7665.

Smith, H. (2000). Phytochromes and light signal perception by plants[mdash]an

emerging synthesis. Nature *407*, 585–591.

Smith, H., and Whitelam, G.C. (1997). The shade avoidance syndrome: multiple responses mediated by multiple phytochromes. Plant, Cell & Environment *20*, 840–844.

Smth, H., and Holmes, M.G. (1977). The Function of Phytochrome in the Natural Environment—iii. Measurement and Calculation of Phytochrome Photoequilibria. Photochemistry and Photobiology *25*, 547–550.

Sozzani, R., Cui, H., Moreno-Risueno, M.A., Busch, W., Van Norman, J.M., Vernoux, T., Brady, S.M., Dewitte, W., Murray, J.A.H., and Benfey, P.N. (2010). Spatiotemporal regulation of cell-cycle genes by SHORTROOT links patterning and growth. Nature *466*, 128–132.

Steindler, C., Matteucci, A., Sessa, G., Weimar, T., Ohgishi, M., Aoyama, T., Morelli, G., and Ruberti, I. (1999). Shade avoidance responses are mediated by the ATHB-2 HD-zip protein, a negative regulator of gene expression. Development *126*, 4235–4245.

Stepanova, A.N., and Alonso, J.M. (2009). Ethylene signaling and response: where different regulatory modules meet. Current Opinion in Plant Biology *12*, 548–555.

Stepanova, A.N., Robertson-Hoyt, J., Yun, J., Benavente, L.M., Xie, D.-Y., Dolezal, K., Schlereth, A., Jürgens, G., and Alonso, J.M. (2008). TAA1-mediated auxin biosynthesis is essential for hormone crosstalk and plant development. Cell *133*, 177–191.

Stokes, T.L., Kunkel, B.N., and Richards, E.J. (2002). Epigenetic variation in Arabidopsis disease resistance. Genes & Development *16*, 171–182.

Tao, Y., Ferrer, J.-L., Ljung, K., Pojer, F., Hong, F., Long, J.A., Li, L., Moreno, J.E., Bowman, M.E., Ivans, L.J., et al. (2008). Rapid synthesis of auxin via a new tryptophan-dependent pathway is required for shade avoidance in plants. Cell *133*, 164–176.

Vandenbussche, F., Pierik, R., Millenaar, F.F., Voesenek, L.A.C.J., and Van Der Straeten, D. (2005). Reaching out of the shade. Curr. Opin. Plant Biol. *8*, 462–468.

Vert, G., and Chory, J. (2006). Downstream nuclear events in brassinosteroid signalling. Nature *441*, 96–100.

Vert, G., Walcher, C.L., Chory, J., and Nemhauser, J.L. (2008). Integration of auxin and brassinosteroid pathways by Auxin Response Factor 2. Proceedings of the National Academy of Sciences *105*, 9829–9834.

Wang, L., Assadi, A.H., and Spalding, E.P. (2008). Tracing branched curvilinear structures with a novel adaptive local PCA algorithm. (Las Vegas, NV: CSREA

Press), p.

Wang, L., Uilecan, I.V., Assadi, A.H., Kozmik, C.A., and Spalding, E.P. (2009). HYPOTrace: image analysis software for measuring hypocotyl growth and shape demonstrated on Arabidopsis seedlings undergoing photomorphogenesis. Plant Physiol *149*, 1632–1637.

Wang, X., and Chory, J. (2006). Brassinosteroids regulate dissociation of BKI1, a negative regulator of BRI1 signaling, from the plasma membrane. Science *313*, 1118–1122.

Wei, N., Serino, G., and Deng, X.-W. (2008). The COP9 signalosome: more than a protease. Trends in Biochemical Sciences *33*, 592–600.

Won, C., Shen, X., Mashiguchi, K., Zheng, Z., Dai, X., Cheng, Y., Kasahara, H., Kamiya, Y., Chory, J., and Zhao, Y. (2011). Conversion of tryptophan to indole-3-acetic acid by TRYPTOPHAN AMINOTRANSFERASES OF ARABIDOPSIS and YUCCAs in Arabidopsis. Proceedings of the National Academy of Sciences of the United States of America.

Wu, G., Cameron, J.N., Ljung, K., and Spalding, E.P. (2010). A role for ABCB19-mediated polar auxin transport in seedling photomorphogenesis mediated by cryptochrome 1 and phytochrome B. Plant J. *62*, 179–191.

Xu, W., Huang, J., Li, B., Li, J., and Wang, Y. (0000). Is kinase activity essential for biological functions of BRI1? Cell Res *18*, 472–478.

Yanagawa, Y., Sullivan, J.A., Komatsu, S., Gusmaroli, G., Suzuki, G., Yin, J., Ishibashi, T., Saijo, Y., Rubio, V., Kimura, S., et al. (2004). Arabidopsis COP10 forms a complex with DDB1 and DET1 in vivo and enhances the activity of ubiquitin conjugating enzymes. Genes Dev. *18*, 2172–2181.

Yang, J., Lin, R., Sullivan, J., Hoecker, U., Liu, B., Xu, L., Deng, X.W., and Wang, H. (2005). Light Regulates COP1-Mediated Degradation of HFR1, a Transcription Factor Essential for Light Signaling in Arabidopsis. Plant Cell *17*, 804–821.

Yang, X., Kuk, J., and Moffat, K. (2009). Conformational differences between the Pfr and Pr states in Pseudomonas aeruginosa bacteriophytochrome. Proceedings of the National Academy of Sciences *106*, 15639–15644.

Yin, Y., Wang, Z.Y., Mora-Garcia, S., Li, J., Yoshida, S., Asami, T., and Chory, J. (2002). BES1 accumulates in the nucleus in response to brassinosteroids to regulate gene expression and promote stem elongation. Cell *109*, 181–191.

Zhang, X., Yazaki, J., Sundaresan, A., Cokus, S., Chan, S.W.-L., Chen, H., Henderson, I.R., Shinn, P., Pellegrini, M., Jacobsen, S.E., et al. (2006). Genome-wide High-Resolution Mapping and Functional Analysis of DNA Methylation in Arabidopsis. Cell *126*, 1189–1201.

Zhao, J., Peng, P., Schmitz, R.J., Decker, A.D., Tax, F.E., and Li, J. (2002). Two putative BIN2 substrates are nuclear components of brassinosteroid signaling. Plant Physiol. *130*, 1221–1229.

Zhao, Y., Christensen, S.K., Fankhauser, C., Cashman, J.R., Cohen, J.D., Weigel, D., and Chory, J. (2001). A role for flavin monooxygenase-like enzymes in auxin biosynthesis. Science *291*, 306–309.